

## Acknowledgements

I would like to express my sincere gratitude to my supervisors Professor Jeremy Roberts and Dr. Chungui Lu who have provided me this great opportunity to study in University of Nottingham. They have given me valuable suggestions and great support during my entire Ph.D study, especially in the thesis correction. I consider myself extremely fortunate for being able to work with them and learn from them. I would also like to express my profound thanks to Dr. Zinnia Gonzalez-Carranza for her help and expert advices in the project and especially in lab-based techniques.

I would also like to thank Xuebin Zhang, Li Zhang and Zubaidh Ramli, Antoine Larrieu, Jie Song and Yu Pan who have given me great help in lab-working. My thanks also go to Dr. Hongying Li, Dr. Ranjan Swarup, Dr. Caiyun Yang, Dr. Zhefeng Lin and Alison Ferguson who have provided lots of experimental materials. Many thanks to Professor Zoe Wilson who have given me positive criticism on this project. I would like to thank everyone in Plant Science Division for helping me in every aspect during my time working here.

Finally, I would like to express my deepest gratitude to my parents for their continuous support and encouragement during this entire Ph.D study.

# Table of Contents

Page

Acknowledgements.....	i
Table of Contents .....	ii
List of Figures .....	vi
List of Tables .....	x
ABBREVIATIONS.....	xi
Abstract.....	xiv

## **CHAPTER 1 General**

<b>Introduction.....</b>	<b>1</b>
--------------------------	----------

<b>1.1 Abscission and Cell separation.....</b>	<b>1</b>
1.1.1 The differentiation of the AZ.....	5
1.1.2 Abscission initiation .....	10
1.1.3 Regulation of cell separation and shedding of organs. ....	21
<b>1.2 The root hair development in <i>Arabidopsis thaliana</i> .....</b>	<b>27</b>
1.2.1 <i>Arabidopsis</i> root hair.....	27
1.2.2 The development of <i>Arabidopsis</i> root hair .....	28
1.2.2.1 The specification of hair-producing cells.....	28
1.2.2.2 The initiation of root hair growth.....	29
1.2.2.3 Tip growth and elongation.....	31
<b>1.3 Aims and objective of the project. ....</b>	<b>35</b>

## **CHAPTER 2 Materials and**

<b>methods.....</b>	<b>38</b>
---------------------	-----------

<b>2.1 Materials .....</b>	<b>37</b>
2.1.1 Plant materials and growth conditions .....	37
2.1.2 Bacterial strains and Plasmid vectors .....	38
2.1.3 Primers .....	39

<b>2.2. Methods</b> .....	<b>42</b>
2.2.1 Growth and maintenance of bacterial strains.....	41
2.2.2 Growing <i>Arabidopsis</i> materials on Murashige and Skoog basal salt mixture (MS) medium .....	41
2.2.3 <i>Arabidopsis</i> crossing.....	42
2.2.4 GUS staining assay .....	43
2.2.5 Genomic DNA isolation.....	43
2.2.6 Polymerase Chain Reaction (PCR) .....	44
2.2.7 RNA isolation and quantitative Reverse-Transcription PCR (qRT-PCR) Analysis.....	45
2.2.8 <i>E. coli</i> DH5 $\alpha$ Transformation with Plasmid DNA .....	48
2.2.9 Purification of Plasmid DNA.....	48
2.2.10 Gateway BP reaction and LR reaction .....	49
2.2.11 <i>Agrobacterium</i> Transformation with Plasmid DNA.....	50
2.2.12 Plant transformation.....	50
2.2.13 Preparation of glycerol stocks.....	51
2.2.14 Annealing of single strand DNA sequences.....	51
2.2.15 Digestion of DNA fragments and plasmids using restriction enzymes.....	52
2.2.16 Dephosphorylation of 5' overhangs .....	52
2.2.17 Ligation of DNA fragments.....	53
2.2.18 Staining <i>Arabidopsis</i> flowers with Synthetic chemical reagent $\beta$ -D-glucosyl Yariv ( $\beta$ -GlcY) .....	53
2.2.9 Immunolocalization .....	54

## **Chapter 3 Expression and Bioinformatic analysis of AT1G64405**

### **(G2).....55**

<b>3.1 Introduction</b> .....	<b>55</b>
<b>3.2 Expression analysis of At1G64405 (G2)</b> .....	<b>66</b>
3.2.1 Analysis of G2: <i>GUS</i> / <i>GFP</i> transgenic lines.....	66
3.2.2 Spatial and temporal G2: <i>GUS</i> expression in three mutants in <i>Arabidopsis</i> .....	74

3.2.2.1 Crossing <i>G2:GUS</i> with <i>inflorescence deficient in abscission (ida)</i>	74
3.2.2.2 Crossing <i>G2:GUS</i> with <i>35S:IDA</i>	75
3.2.2.3 Crossing <i>G2:GUS</i> with <i>blade-on-petiole1 &amp; blade-on-petiole2 (bop1/bop2)</i>	76
3.2.2.4 Wounding-related expression of <i>G2:GUS</i>	79
<b>3.3 Bioinformatic analysis of G2 gene and protein</b>	<b>83</b>
3.3.1 G2 gene expression pattern predicted by Genevestigator_V3	86
3.3.2 Identification of putative orthologues of G2	89
3.3.3 Four motifs of G2 protein were shown to be conserved among 19 deduced proteins from different plant species.	92
3.3.4 Protein secondary structure analysis	98
3.3.5 G2 protein sequence has 2 motifs in N' and C' terminal that are conserved with 9 <i>Arabidopsis thaliana</i> proteins.	101
<b>3.4 Discussion</b>	<b>104</b>
3.4.1 Identification of G2 as an abscission-related gene	104
3.4.2 The expression of G2 is correlated with the expression shows an inverse correlation with <i>IDA</i> .	106
3.4.3 Transcription analysis of G2 in <i>Arabidopsis</i> and sequence analysis of G2 with putative orthologues in other species	108
3.4.4 Identification of 9 potential orthologues of G2 from <i>Arabidopsis thaliana</i> .	111

## **Chapter 4 Functional analysis of**

### **G2.....113**

<b>4.1 Manipulation of G2 Expression</b>	<b>113</b>
4.1.1. Generation of G2 null lines using a T-DNA strategy	114
4.1.2. Generation of G2 null lines using an RNAi strategy	116
4.1.3. Generation of ectopically expressing lines of G2	121
<b>4.2 Characterization of Knock Out and overexpression lines of G2 and analysis of phenotypes</b>	<b>125</b>
4.2.1 Phenotypes of <i>RNAi:G2</i> plants	126
4.2.2 Phenotype of <i>35S:G2</i>	127
<b>4.3 Crossing 35S:G2 with 35S:IDA</b>	<b>135</b>
4.3.1 Screening and isolation of homozygous lines of <i>35S:G2</i> × <i>35S:IDA</i> .	136

4.3.2 Phenotype of 35S: <i>IDA</i> x 35S: <i>G2</i> lines .....	137
4.3.3 35S: <i>IDA</i> x 35S: <i>G2</i> homozygous plants were observed to be normal in morphology and development compared to 35S: <i>IDA</i> .....	146
4.3.4 35S: <i>IDA</i> rescues the phenotype of swelling root hairs of 35S: <i>G2</i> .	148
4.3.5 Immunolocalization of 35S: <i>G2</i> root hairs .....	151
4.3.6 <i>Generation of a translational fusion by fusing G2 protein with GFP.</i> .....	152

<b>4.4 Discussion.....</b>	<b>157</b>
4.4.1 Generation and analysis of lines down-regulated in the expression of <i>G2</i> .....	157
4.4.2 Overexpression of <i>G2</i> in 35S: <i>IDA</i> background rescues the effects of 35S: <i>IDA</i> in floral organ abscission .....	159
4.4.3 Overexpression of <i>G2</i> leads to swollen root hairs.....	162

## ***Chapter 5 Promoter analysis in Abscission-related***

<b><i>genes.....</i></b>	<b>174</b>
--------------------------	------------

<b>5.1 Introduction.....</b>	<b>174</b>
5.1.1 Promoter .....	174
5.1.2 Transcription factor (TF) .....	175
5.1.3 Abscission-related transcription factors .....	175
5.1.4 Promoter analysis .....	176
<b>5.2 Results.....</b>	<b>177</b>
5.2.1 Identification of the 10 bps motif .....	177
5.2.2 Analysis of the function of the motif AATATACATT.....	179
<b>5.3 Discussion and future work.....</b>	<b>184</b>
5.3.1 Identification of potential abscission-related motifs.....	184

## ***Chapter 6 Conclusion and future work.....***

<b><i>Reference.....</i></b>	<b>191</b>
------------------------------	------------

# List of Figures

	<u>Page</u>
<b>Figure 1.1</b> A proposed flowchart of the chain of events that take place and the genes expression changes at different stages during abscission process in <i>Arabidopsis</i> .	5
<b>Figure 1.2</b> Diagrams of the abscission zone of a leaf.	6
<b>Figure 1.3</b> The abscission zone cells marked with GFP	37
<b>Figure 3.1:</b> Functional categorization of the fifty most highly expressed genes which were selected from a cDNA library generated from the AZ Micro array data	57
<b>Figure 3.2:</b> GUS expression in the abscission zone of the flowers at position 7 - 10 of the 6 genes.	62
<b>Figure 3.3:</b> RT-PCR analysis to identify knockouts of the genes <i>At3g56350</i> , <i>At1g64405</i> , <i>At2g23630</i> and <i>At3g53040</i>	64
<b>Figure 3.4</b> <i>G2:GFP</i> and <i>G2:GUS</i> expression in the abscission zone of the flower at position 8 and position 10 of <i>Arabidopsis</i> .	67
<b>Figure 3.5</b> Time course of <i>G2:GUS</i> expression.	69
<b>Figure 3.6:</b> Confocol imaging of the time coursed <i>G2:GFP</i> expression	71
<b>Figure 3.7:</b> <i>G2:GFP</i> expression in root tissue	73
<b>Figure 3.8</b> Time course of <i>G2</i> expression during flower development	78
<b>Figure 3.9</b> Wound-induced expression of <i>G2:GUS</i> in a cauline leaf	79
<b>Figure 3.10</b> wound-induced expression of <i>G2:GUS</i> ( <i>Pro<sub>At1g64405</sub>:GUS</i> ) in different genetic backgrounds.	80
<b>Figure 3.11</b> <i>G2:GUS</i> expression in roots tissues in the wild type, <i>ida</i> and <i>35S:IDA</i> backgrounds.	82
<b>Figure 3.12</b> NASC array Two Genes Scatter Plot of the correlation between <i>G2</i> and <i>IDA</i> .	84

<b>Figure 3.13</b> G2:GUS expression in the root tips of wild type, ida and 35S:IDA backgrounds.	85
<b>Figure 3.14</b> G2 expression value in different tissues in <i>Arabidopsis</i> from Genevestigator V3 (Anatomy).	88
<b>Figure 3.15</b> G2 expression pattern at different developmental stages shown by Gene Chronology tool from Genevestigator_V3.	88
<b>Figure 3.16</b> ClustalW alignments of the deduced amino acid from the translation start sites of ORF among G2 and four proteins from <i>Brassica</i> , <i>Raphanus raphanistrum</i> , and <i>Raphanus sativus</i> respectively.	90
<b>Figure 3.17</b> ClustalW alignment of the deduced amino acid from the translation start sites of ORF among G2 and nineteen genes from different species.	93
<b>Figure 3.18</b> Amino acids scales of hydrophobicity of the twenty deduced proteins sequences from Prot Scale tools of ExPASy.	97
<b>Figure 3.19</b> Predicted secondary structure of the twenty proteins with the background of ClustalW alignments.	100
<b>Figure 3.20</b> A cartoon picture of the 3D structure of the deduced protein of <i>Zea mays</i> predicted by PHYRE server.	100
<b>Figure 3.21</b> ClustalW alignment of the deduced amino acid from the translation start sites of ORF among G2 and nine genes from <i>Arabidopsis</i> .	102
<b>Figure 4.1</b> A schematic diagram of T-DNA insertion positions of G2.	114
<b>Figure 4.2</b> PCR analysis of putative T-DNA insertion lines (SALK_565404) of G2.	115
<b>Figure 4.3</b> PCR analysis of putative T-DNA insertion lines (SALK_55356) of G2.	115
<b>Figure 4.4</b> RT-PCR analysis of putative T-DNA insertion lines SALK_065404 and SALK_055356..	116
<b>Figure 4.5</b> Diagram of GateWay <sup>TM</sup> pDONR <sup>TM</sup> 221 entry vector.	117
<b>Figure 4.6</b> Schematic diagram of G2Entry plasmid construct.	118
<b>Figure 4.7</b> PCR analysis of the colonies that contain the G2Entry plasmid using primers M13_Forward and G2_reverse.	118

<b>Figure 4.8</b> The G2 cDNA fragment in the Entry Clone was transferred to a destination vector, pK7GWIWG2.	119
<b>Figure 4.9</b> PCR analysis of plasmids from the two colonies transformed with <i>Agrobacterium tumefaciens</i> C58.	120
<b>Figure 4.10</b> RT-PCR analysis of <i>RNAi:G2</i> Plants.	121
<b>Figure 4.11.</b> The G2 fragment in the Entry Clone was transferred to a destination vector, pGWB8.	122
<b>Figure 4.12</b> PCR analysis of plasmids from the six colonies of transformed <i>Agrobacterium tumefaciens</i> C58.	123
<b>Figure 4.13</b> RT-PCR analysis of 35S:G2 Plants. Group Gene Specific shows the RT-PCR product amplified using primer G2_Forward and G2_Reverse.	124
<b>Figure 4.14</b> Undeveloped seeds identified in siliques of <i>RNAi:G2</i> and wild type and the percentage of fully developed seeds.	126
<b>Figure 4.15</b> Pollen of <i>RNAi:G2</i> and wild type stained with Alexander solution.	127
<b>Figure 4.16</b> Phenotypic analysis of the roots of wild type and 35S:G2.	129
<b>Figure 4.17</b> Phenotype of wild type and 35S:G2 root hairs. 7 day old <i>Arabidopsis</i> roots were analysed under the microscope.	131
<b>Figure 4.18</b> The diameters of 35S:G2 type I, type II and type III root hairs. The diameters were determined by calculating the average diameter of thirty root hairs.	132
<b>Figure 4.19</b> The length of 35S:G2 type I, type II and type III root hairs.	133
<b>Figure 4.20</b> The density of 35S:G2 and wild type root hairs in the elongation zone.	134
<b>Figure 4.21</b> Genomic PCR to select F2 generation of 35S:G2 x 35S:IDA.	137
<b>Figure 4.22</b> Genomic PCR to select F3 homozygotes of 35S:G2 x 35S:IDA (line B13).	137
<b>Figure 4.23</b> Time course analysis of floral organ abscission of wild type (WT), 35S:G2, 35S:IDA and 35S:IDA x 35S:G2 plants.	139



<b>Figure 4.24</b> Floral AZ of wild type 35S:G2, 35S:IDA and 35S:IDA x 35S:G2.	140
<b>Figure 4.25.</b> Identification of Arabinogalactan using the Yariv Reagent $\beta$ -GlcY.	142
<b>Figure 4.26</b> RT-PCR of mRNA from both flowers (P5 – P8) and cauline leaves.	145
<b>Figure 4.27</b> Phenotypes of whole plants of wild type, 35S:G2, 35S:IDA and 35S:IDA x 35S:G2.	147
<b>Figure 4.28</b> <i>Arabidopsis</i> root hairs.	148
<b>Figure 4.29</b> The morphology of rosette leaves ( <b>Group A</b> : whole seedlings, <b>Group B</b> : rosette leaves from the same position).	150
<b>Figure 4.30:</b> Immunolocalization of the root hair tissue of wild type (W.T.) and 35S:G2	152
<b>Figure 4.31:</b> Schematic diagram of G2Entry plasmid construct.	153
<b>Figure 4.32:</b> PCR analysis of the colonies that contain the PrG2Entry plasmid using primers PrG2_Forward and M13_reverse.	154
<b>Figure 4.33:</b> The fragment in the Entry Clone PrG2Entry was transferred to a destination vector, pGWB4	155
<b>Figure 4.34</b> PCR analysis of plasmids from the 4 colonies of transformed <i>Agrobacterium tumefaciens</i> C58	156
<b>Figure 4.35</b> Genevestigator V3 result of the expression value of <i>AGP24</i> in tissues of <i>Arabidopsis</i> .	164
<b>Figure 4.36</b> Genevestigator result of the expression value of <i>At/DL1</i> in tissues of <i>Arabidopsis</i> .	166
<b>Figure 4.37</b> Root hair of 35S:IDA plant. Yellow arrow points to a normally developed hair. White arrow points to a branched hair	170
<b>Figure 4.38</b> Proposed model of how overexpression of G2 leads to the swollen, crooked and branched phenotypes.	173
<b>Figure 5.1</b> The location of the motif <b>AATATACATT</b> in the abscission-related genes.	177

<b>Figure 5.2</b> The picture shows the genes that are shared between the micro-array data and the PetMatch BLAST result.	179
<b>Figure 5.3</b> The 10bp motif AATATACATT was transformed into MOG257 vector.	180
<b>Figure 5.4</b> PCR for selection of the colonies that contain the RP1:GUS ,RP2:GUS and RP3:GUS using primers MOGForward and GUSSequece.	182
<b>Figure 5.5</b> PCR analysis of plasmids from the colonies transformed into <i>Agrobacterium tumefaciens</i> C58.	182
<b>Figure 5.6</b> PCR analysis of the primary transformatants using primers MOG_Forward and GUS_Sequence.	183

## List of tables

<b>Table 1.1</b> Primers used in this project.	41
<b>Table 1.2</b> The expression information and putative functions of the six genes selected from the micro array data	49
<b>Table 1.3</b> Equation to quantify the amount of DNA added into the ligation reaction.	53
<b>Table 3.1</b> TBLASTX analysis result using G2 nucleotide sequence as a probe.	90

## ABBREVIATIONS

A	alpha
$\beta$	beta
$\mu\text{g}$	microgram
$\mu\text{l}$	microlitre
$\mu\text{m}$	micrometer
$\mu\text{mol}$	micromole
aa	amino acid
ABA	abscisic acid
ACC	1-aminocyclopropane
AMP	ampicillin
ATG	translation start codon
AZ	abscission zone
Bp	base pair
$^{\circ}\text{C}$	degrees centigrade
CaMV35S	Cauliflower mosaic virus 35S
cDNA	complementary DNA
CL	cauline leaves
cm	centimetre
Col-0	columbia-0-wild type
DDW	double distilled water
DNA	deoxyribose nucleic acid
DNase	deoxyribonuclease

dNTP	deoxyribonucleoside triphosphate
dATP	2'-deoxyadenosine 5'-triphosphate
dCTP	2'-deoxycytosine 5'triphosphate
dGTP	2'-deoxyguanosine 5'-triphosphate
dTTP	2'-deoxythymidine 5'-triphosphate
EDTA	diamino ethanetetra-acetic acid
<i>E. coli</i>	<i>Escherichia coli</i>
<i>et al</i>	<i>et alia</i> (and others)
g	gram
Kb	kilobase
KO	knock out
L	litre
LB	luria-bertani
m	metre
Mb	mega base pairs
min	minute
ml	millilitre
mM	millimolar
mg	milligram
mRNA	messenger ribonucleic acid
MS	murashige and skoog basal
ng	nanogram
OD	optical density
ORF	open reading frame
RNA	ribonucleic acid

RNase	ribonuclease
RNAi	ribonucleic acid interference
s	second
SDS	sodium dodecyl sulphate
SDW	sterile distilled water
SEM	scanning electron microscopy
Taq	Taq polymerase
TBE	Tris-borate-EDTA
T-DNA	transfer DNA
Tris	Tris (hydroxymethyl) methylamine
UTR	untranslated region
UV	ultra violet
V	voltage
vol	volume
v/v	volume per volume
WT	wild type
w/v	weight per volume
X-Gluc	5-bromo-4-chloro-3-indolyl-beta-D-glucuronic acid

## Abstract

Abscission is an important process in the life cycle of a plant. It takes place in predetermined sites called Abscission Zones (AZs). In the previous study of our group, a potential abscission-related gene *At1g64405* (*G2*) was identified of particular interest using a transcriptional analysis. The aim of this study was to characterize this gene in detail.

Expression analysis of *G2* was carried out by fusing its promoter with *GUS* or *GFP*. Reporter gene expression was detected specifically in floral organ AZ and cortical cells surrounding the sites of lateral roots emergence. Crosses were then carried out between *G2:GUS* plants and three important abscission mutants: *ida*, *35S:IDA* and *bop1/bop2* in order to further investigate the expression pattern of *G2*. The results, together with the bioinformatics analysis, indicate that *G2* is specifically expressed in AZ and is an abscission-related gene, and reveal an inverse correlation between the expression of *G2* and *IDA*. A gene manipulation strategy was then undertaken to generate the ectopically expressed and silenced lines of *G2*. Overexpression of *G2* was achieved by fusing *G2* to a 35S promoter whereas the null lines were obtained by an RNAi strategy. *35S:G2* plants displayed unusual root hair morphology while down-regulating *G2* generated plants where pollen partially failed to develop. *35S:IDA* mutants displayed phenotypes with earlier abscission, extended AZ, and the ectopic secretion of AGPs at the site of organ shedding.

Ectopic expression of *G2* in *35S:IDA* plants partially suppressed these features. A bioinformatics analysis was performed to study *G2* protein sequence in order to find out potential functional domains and four motifs were selected that may be important for protein function. The potential role of *G2* will be discussed in detail in this thesis.



# **CHAPTER 1**

## **General Introduction**

### **1.1 Abscission and Cell separation**

A plant will abscise an organ for many reasons. 1) An organ might be shed once it is no longer needed, such as floral organs after fertilization, leaves during the autumn and fruits after ripening. 2) The shedding of an organ can also be benefit for recycling substances for the generation of energy. Organs towards the end of their life are large mineral sinks, and their abscission can allow photosynthates and nutrients to supply other organs. 3) Plants may shed their organs in

order to adapt to a change in the environment such as the changing of day length or temperatures (Taylor and Whitelaw, 2001). For example, deciduous trees lose their leaves in the autumn in order to survive during the winter months when water supplies are limited while evergreen plants continuously abscise their leaves. 4) A plant will also prematurely drop an organ which has been infected by a pathogen in order to prevent spreading of the disease. Once shed, a protective scar develops at the abscission site to protect against pathogen attack (Taylor and Whitelaw, 2001; Roberts *et al.*, 2002). 5) A plant will also abscise organs to enhance reproductive success such as that ripened fruit are shed to disperse seeds for the next generation. 6) Plants may shed organs to avoid competition for resources. For instance, some plants species drop leaves that contain toxic chemicals that can inhibit the growth of other plants.

Although the phenomenon of shedding entire organs in animals - for example, antler shedding in deer, skin shedding in snakes, tail autotomy in lizard - is less common than in plants, they share some similar features such as the separation happens in specific cell layers and is coordinated by enzymes that dissolve cell to cell adhesion (Leslie *et al.*, 2007).

The shedding of plant organ is also known as abscission which has been well documented for thousands of years. For the benefits of agriculture, farmers have been selecting desired traits of different crops for centuries. During the long term domestication of crops, one of the key traits points for increasing yield was to reduce the shedding of seeds. Humans have made significant achievement through thousands of years. For example, the modern maize was domesticated from a wild grass, teosinte (Paul, 1974). A key difference is that the ears of domesticated maize remain intact until harvest. Another example is that the discovery of genes such as *JOINTLESS* in tomato and the introgression of this trait into other tomato cultivars provides another excellent example of human-directed evolution of crop species and it has been widely used in the processing tomato industry (Mao, *et al.*, 2000).

Abscission is a phenomenon that involves cells separation. Cell separation is a critical process that takes place throughout the life cycle of a plant (Roberts *et al.*, 2002). It enable roots to appear from a germinating seed, cotyledons and leaves to expand, pollen to be released, fruit to soften, and organs to be shed (Hawes and Lin, 1990; Sitrit *et al.*, 1999; Chen and Bradford, 2000; Roberts and González-

Carranza, 2007). During cell separation, the cell wall is degraded. Although the biochemical processes that lead to wall breakdown may be comparable, the nature of the signals that induce these changes are likely to be different so that the process only occurs at critical spatial and temporal locations (Roberts *et al.*, 2002).

*Arabidopsis thaliana* has been shown to be an excellent model species to study plant development. Although *Arabidopsis* plants do not shed their leaves, it is very effective to use it as subject of forward genetic screens in the search for phenotypes that fail to shed floral organs or seeds (Patterson, 2001). The chain of events of abscission in *Arabidopsis* can be divided into 4 parts, (1) the differentiation of the AZ, (2) abscission initiation, (3) expression of abscission-related genes, and (4) the shedding of organs (Roberts *et al.*, 2002). Every part is induced by certain factor(s), regulated by different hormones/genes and accompanied by changes in gene expression (Figure 1.1). The detail of each part/factor will be discussed in the following paragraphs.

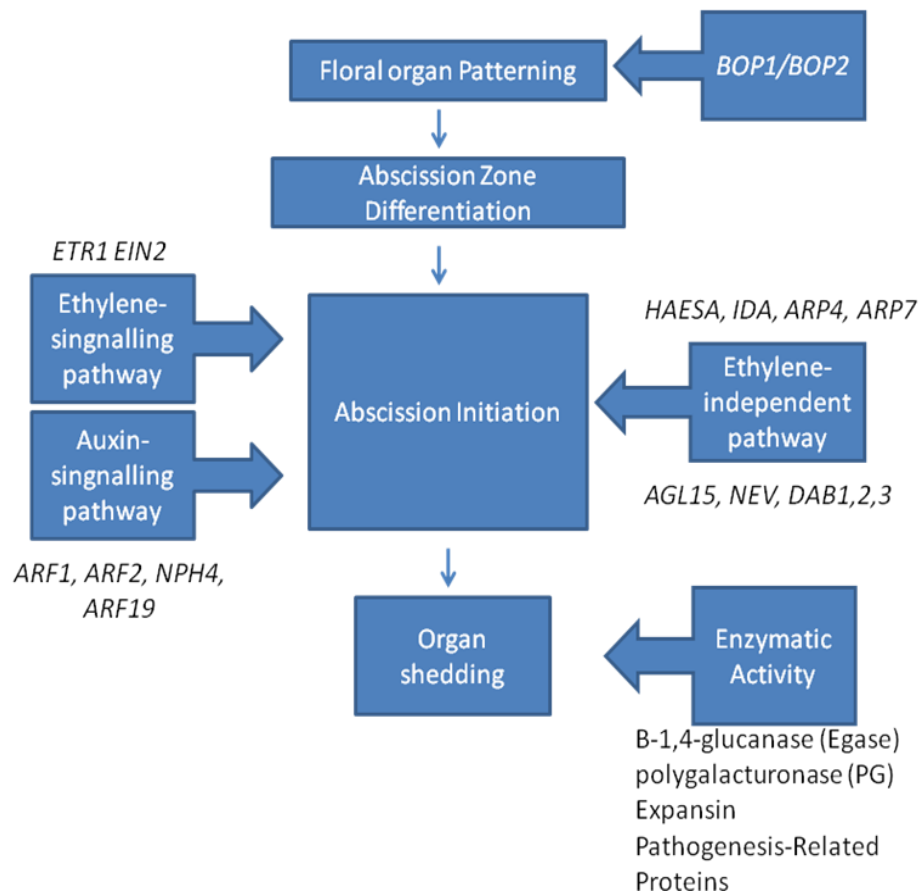


**Figure 1.1** A proposed flowchart of the chain of events that take place and the genes expression changes at different stages during abscission process in *Arabidopsis*.

### 1.1.1 The differentiation of the AZ

The shedding of a plant organ takes place at predetermined positions called abscission zones (AZs) (Sexton and Roberts, 1982). AZs are commonly predetermined sites that are located at the base of organs such as flowers, fruit, leaf and seed, and can frequently be morphologically identified as being isodiametric cells that are cytoplasmically dense, and usually smaller and more closely packed

than the surrounding cells (Bleecker and Patterson, 1997; Roberts *et al.*, 2002) (Figure 1.2). During the process of abscission, the middle lamella is degraded and is accompanied by the rearrangement of cellulose microfibrils (Patterson *et al.*, 1996). Golgi activity has been shown to increase and the endomembrane system is activated in AZ cells (Sexton and Roberts, 1982). It has also been reported that AZ cells show a different response to hormone signals compared to adjacent cells (Taylor and Whitelaw, 2001).

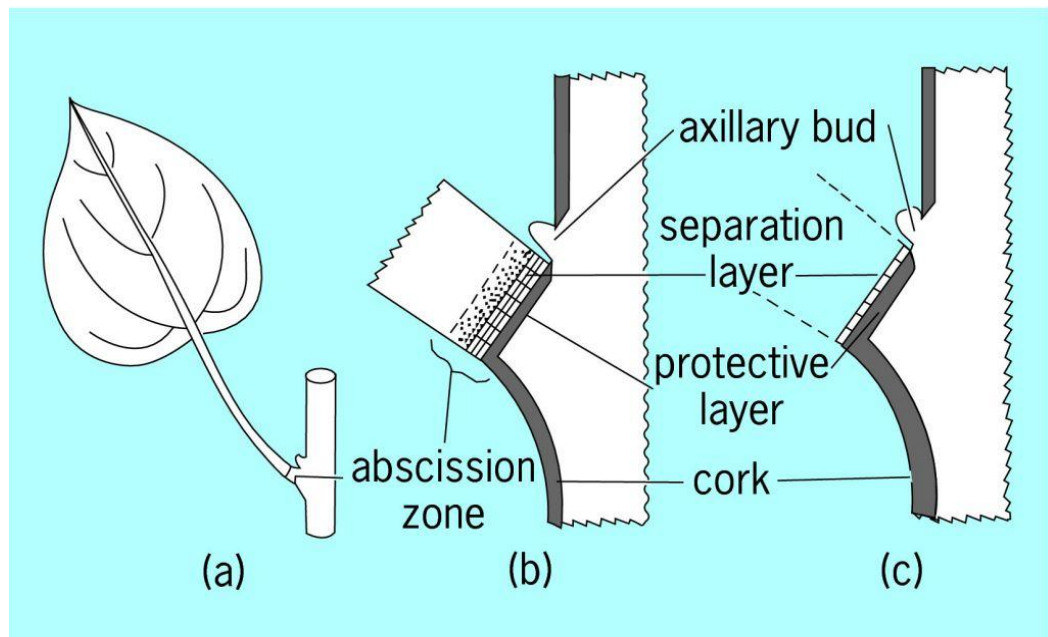


**Figure 1.2** Diagrams of the abscission zone of a leaf. (a) A leaf with the abscission zone indicated at the base of the petiole. (b) The abscission zone layers shortly before abscission and (c) the layers after abscission.

([http://encyclopedia2.thefreedictionary.com/\\_/viewer.aspx?path=mgh\\_ceb&name=Diagrams-of-the-abscission-zone-of-a-leaf.jpg](http://encyclopedia2.thefreedictionary.com/_/viewer.aspx?path=mgh_ceb&name=Diagrams-of-the-abscission-zone-of-a-leaf.jpg))

The regulatory mechanisms controlling AZ formation and separation will be discussed in the following paragraph.

Before organ separation takes place, a plant needs to develop an AZ, which could be accomplished up to several months before organ separation actually takes place. A number of genes have been shown to be involved in this process.

The MADS-box family of transcription factors has been shown to play an important role in the establishment of specific sites of cell differentiation in tomato (Mao *et al.*, 2000), and some MADS-box genes have been shown to play an important role in flower organogenesis in *Arabidopsis* which are discussed below (Honma and Goto, 2001; Pelaz *et al.*, 2001).

### **JOINTLESS**

In tomato, the gene *JOINTLESS* (*J*), which encodes a MADS-box domain transcription factor, has been identified by map-based cloning. *JOINTLESS* is expressed strongly in flower meristem and the mutant *j* in tomato does not develop a pedicel AZ and also fails to shed its flowers and fruits (Mao *et al.*, 2000). This trait has been bred into

tomato as it is agronomically desirable to facilitate the harvesting and transport of fruit. *J* has been shown to mediate cell to cell signalling which is critical for inflorescence patterning and AZ differentiation (Szymkowiak and Irish, 1999), however how the *J* signal is communicated remains unclear (Szymkowiak and Irish, 1999).

### **SEEDSTICK**

An *Arabidopsis* seed is attached to the funiculus, and the seed AZ, which differentiates after fertilization, is a layer of distinctly small cells closely adjacent to the seed (Pinyopich *et al.*, 2003). Another MADS-BOX domain transcription factor, *SEEDSTICK* (*STK*) has been identified to play an important role in funicular patterning (Pinyopich *et al.*, 2003). Plants with a non-functional *STK* develop an enlarged funiculus which prevents seed abscission (Pinyopich *et al.*, 2003).

### **BLADE ON PETIOLE 1 AND 2**

In *Arabidopsis*, the *BLADE ON PETIOLE1 and 2* (*BOP1* and *BOP2*) have been reported to play an important role in AZ differentiation in *Arabidopsis* (Hepworth *et al.*, 2005, McKim *et al.*, 2008). Single loss-of-function mutations of either *BOP1* or *BOP2* do not show any



phenotypic difference comparing to wild type, however the absence of both *BOP1* and *BOP2* leads to a failure in AZ formation and as a consequence floral organs are not shed. *BOP1* and its closely related gene *BOP2* are members of NONEXPRESSOR OF PATHOGENESIS-RELATED GENES 1 (NPR1) family of transcription factors (Ha *et al.*, 2004). *NPR1* is a positive regulator of systemic acquired resistance (SAR), a plant immune response induced following local infection (Durrant and Dong, 2004). It has been shown that *BOP1* and *BOP2* act in cells adjacent to the lateral organ boundary to repress genes that confer meristem cell fate and induce genes that promote lateral organ fate and polarity (Ha *et al.*, 2007). The expression analysis shows that at the beginning of flower development, *BOP1* and *BOP2* are expressed in the proximal regions of floral organs (Ha *et al.*, 2007). Then, as the development of the flower progress, both of the genes are expressed in regions overlapping with the flower AZ. *BOP1* and *BOP2* negatively regulate expression of class I knox genes, *BREVIPEDICELLUS* (*BP*), *KNAT2*, and *KNAT6* in the bases of developing leaves, and positively regulate *LATERAL ORGAN BOUNDARIES* (*LOB*) domain (*LBD*) gene expression (Lewis *et al.*, 2005). Further studies have been carried out to analyse additional activities of *BOP1* and *BOP2*. McKim *et al.* (2008) characterized the

*bop1/bop2* abscission phenotype and demonstrated that BOP proteins are essential for the establishment of AZ cells in different tissues. *BOP1/BOP2* activity is required for both premature floral organ abscission and the ectopic abscission of cauline leaves promoted by the overexpression of *INFLORESCENCE DEFICIENT IN ABSCISSION (IDA)*, which suggests that due to the disruption in AZ architecture in *bop1/bop2*, ectopic expression of *IDA* is not sufficient to promote abscission. The expression of several important abscission-related genes, *IDA*, *HAESA* and *HAWAIIAN SKIRT* were investigated in *bop1/bop2* background and the results showed that they had the same expression level compared to wild type (McKim *et al.*, 2008). Finally, the *BOP* genes were shown to be essential for AZ formation in *Arabidopsis*, and their activity is required for multiple cell differentiation events in the proximal regions of lateral organs in the inflorescence (McKim *et al.*, 2008).

### **1.1.2 Abscission initiation**

After the differentiation of the AZ, the next event is the triggering of the cells that make up the AZ so that cell wall degradation takes place. The time from the differentiation of AZ to the shedding of organ is dependent on environmental conditions. It may be closely linked in

organs such as flowers, or separated by many months between the two processes, for example, in leaves. A key question that has been proposed is what factor(s) are responsible for regulating the timing of cell separation, and are they different or comparable at various abscission sites?

### **Ethylene-signalling pathway**

Ethylene has been shown to play an important role in plant developmental process such as germination, ripening, senescence, responses to stress, and abscission. Early studies support the model that ethylene promotes cell separation whereas auxin delays this process (Sexton and Roberts, 1982). To accelerate cell separation, continuous exposure to ethylene is needed (Sexton and Roberts, 1982). It has been shown that ethylene induces the synthesis and secretion of some cell wall and middle lamella hydrolytic enzymes which are needed for cell separation and the abscission process (Tucker *et al.*, 1991; Kalaitzis *et al.*, 1997; Burns *et al.*, 1998). Some genes have been identified that are involved in the ethylene-signalling pathway and have a significant effect on the timing of abscission.

The “triple response” caused by exposure of dark grown seedlings to ethylene has been used in screening *Arabidopsis* genes involved in the ethylene-signalling pathway (Alonso and Stepanova, 2004; Guo and Ecker, 2004). *ETHYLENE RECEPTOR 1 (ETR1-1)* was the first gene identified to play a role in ethylene-signalling pathway. *etr1-1* mutations show no sensitivity to ethylene and exhibit a delay in the shedding of floral organs in *Arabidopsis* (Bleecker and Patterson, 1997, Chao *et al.*, 1997). *ETR1* encodes an ethylene receptor and has been localised to the endoplasmic reticulum (ER) and binds ethylene at its N-terminus (Chen *et al.*, 2002; Guo and Ecker, 2004).

Another gene, *ETHYLENE-INSENSITIVE2 (EIN2)* has also been demonstrated to be required for the “proper” timing of abscission. The *ein2* mutant exhibits a strong ethylene-insensitive phenotype and floral organ abscission is not accelerated by exposure to ethylene (Chao, *et al.*, 1997). *EIN2* has been predicted to be localised to the ER membrane and function downstream and interact with *ETR1* (Bisson, *et al.*, 2009). Loss-of-function mutation of either *ETR1* or *EIN2* in *Arabidopsis* will prevent floral organs from shedding until sepals and petals have begun to wither (Patterson, 2001; Patterson and Bleecker, 2004).

Four *ETR1*-related genes *ETHYLENE RESPONSE SENSOR 1* (*ERS1*), *ETR2*, *ETHYLENE-INSENSITIVE 4* (*EIN4*), and *ERS2* have been identified based on their sequence similarities (Hua *et al.*, 1995; Hua *et al.*, 1998; Sakai *et al.*, 1998). Together with *ETR1* they have been classified into two subfamilies: (1) *ETR1* and *ERS1* and (2) *ETR2*, *EIN4* and *ERS2*. Plants with single loss-of-function of *ETR1*, *ETR2*, *EIN4*, *ERS1* and *ERS2* did not show any defects in ethylene response, while triple *etr1*, *etr2* and *ein4*, and quadruple *etr1*, *etr2*, *ein4* and *ers2* null mutants display ectopic response in the absence of ethylene, suggesting that they have redundant functions in ethylene signalling (Hua and Meyerowitz, 1998; Qu *et al.*, 2008). Further analysis has shown that plants with double mutation in *ETR1* and *ERS1* display constitutive ethylene-response phenotype which is more pronounced than other ethylene receptors mutations combinations, suggesting that subfamily (1) plays an predominant role in regulating the ethylene signalling (Liu *et al.*, 2010).

The tomato gene *NEVER-RIPE* (*NR*) encodes an ethylene receptor orthologous to the *Arabidopsis* gene *ETR1* (Rick and Butler, 1956; Lanahan *et al.*, 1994). It has been shown that *nr* mutations exhibit a delay in senescence, fruit ripening and pedicel abscission (Rick and

Butler, 1956; Lanahan *et al.*, 1994). The study also found that ethylene treatment did not cause significant effect in the acceleration of abscission in flower explants (Lanahan *et al.*, 1994). Further work has revealed that *NR* functions through its inhibitory role in ethylene signal transduction (Hackett *et al.*, 2000).

### **Ethylene-independent-signalling pathway**

In ethylene-insensitive mutants, abscission is considerably delayed, but does eventually take place, which suggests that ethylene signalling is important for the timing of abscission but is not the only regulatory factor (Patterson and Bleecker, 2004).

### ***INFLORESCENT DEFICIENT IN ABSCISSION***

The *INFLORESCENT DEFICIENT IN ABSCISSION (IDA)* gene encodes a protein in *Arabidopsis* that is crucial for floral organ shedding. It was isolated by a T-DNA strategy and found to encode a putative secreted peptide ligand suggested to act late in abscission to promote middle lamellae dissolution (Butenko *et al.*, 2003). In *ida* mutants, floral organs remain attached to the plant body after the shedding of mature seeds, even though a floral AZ develops (Butenko

*et al.*, 2003). Reporter gene analysis has shown that IDA is expressed specifically in AZ cells of floral organs. By fusing the *IDA* promoter with GUS, *IDA:GUS* expression pattern was congruent with timing and phenotypic changes seen in the *ida* mutant (Butenko *et al.*, 2003). The product of the translational fusion of *IDA:GFP* has been detected in the extracellular space which suggests that IDA might act as a signal peptide (Butenko *et al.*, 2003). It was also shown that IDA acts after differentiation of the floral abscission zone. A breakstrength analysis revealed that the breakstrength of petals increased in the mutant background after the shedding of floral organs in wild-type plants, which demonstrated that IDA may play an important role in one of the final processes of abscission (Butenko *et al.*, 2003). Compare to other ethylene-insensitive mutants, *ida* plants exhibit a wild-type phenotype in response to ethylene exposure at other stages of development including the triple response. When treated with ethylene, *ida* flowers senesce rapidly but are not shed (Butenko *et al.*, 2003). In ectopically expressing *IDA* transgenic lines (35S:*IDA*) AZ cells proliferated and are accompanied by excessively secreted Arabinogalactan-protein (AGP), and abscission of floral organs occurs prematurely, suggesting that the AZs are responsive to *IDA* soon after the opening of the flowers (Stenvik *et al.*, 2006).

Sequence homologies have revealed that *IDA* belongs to a family of putative ligands and similar phenotype of *35S:IDA* was detected in plants ectopically expressing *IDA-LIKE (IDL)* genes (Butenko *et al.*, 2003; Stenvik *et al.*, 2008). A C-terminal motif EPIP was identified to be conserved among *IDA* and *IDL* protein sequences and this motif was shown to partially substitute for *IDA* function (Stenvik *et al.*, 2008). Further analysis predicted that *IDA* could be functionally dependent on the presence of the receptor like protein kinase (RLKs) *HAESA* and *HAESA-LIKE2 (HSL2)* (Stenvik *et al.*, 2008).

### ***HAESA***

*HAESA (HAE)*, which is thought to be targeted to the plasma membrane, belongs to the leucine-rich repeat (LRR) class of RLKs and the expression analysis showed that *HAE* is specifically expressed in floral organs in *Arabidopsis* (Jinn, *et al.*, 2000). Down-regulation of *HAE* expression using an antisense RNA strategy leads to a failure of floral organ abscission in *Arabidopsis* (Jinn *et al.*, 2000). *HAE* was predicted to function in an ethylene-independent pathway in abscission because the expression of the gene was not affected by treatment with ethylene (Jinn, *et al.*, 2000). The non-shedding phenotype of the



*haesa/hsl2* double mutant could not be rescued by ectopically expressing *IDA*, which suggests that *HAESA* and *HSL2* are epistatic to *IDA* (Stenvik *et al.*, 2008). Further study by Cho *et al.* (2008) showed that *MITOGEN-ACTIVATED PROTEIN KINASE 4* (*MKK4*), *MKK5* and *MKK6* were acting downstream of *IDA* and *HAE* and constitutive expression of the *MKKs* could rescue the abscission effect of *hae/hsl2* and *ida* mutants. *IDA*, *HAESA* and *HSL2* have been predicted to function in a common pathway and *IDA* and *IDL* proteins have been proposed to act through RLKs in regulating other processes during plant development (Stenvik *et al.*, 2008).

### ***NEVERSHED and EVERSHED***

Recently, the gene *NEVERSHED* (*NEV*) has been reported to play an important role in cargo molecule trafficking required for cell separation in *Arabidopsis* and a mutation of *NEV* prevents floral organ shedding (Liljegren *et al.*, 2009). *NEV* encodes an ADP-ribosylation factor GTPase-activating protein and *NEV* is located in the trans-Golgi network and endosomes in *Arabidopsis* root epidermal cells (Liljegren *et al.*, 2009). In the absence of *NEV* plants show defects in Golgi structure apparatus and extensive accumulation of vesicles adjacent to the cell walls (Liljegren *et al.*, 2009).

The gene *EVERSHED* (*EVR*) encodes a leucine-rich repeat receptor-like kinase (LRR-RLK) and was identified in a screen of mutations that can rescue the phenotype of the *nev* mutants. This discovery suggests that *EVR* also plays an important role in membrane trafficking (Leslie *et al.*, 2010). The double knock out mutants *nev/evr* display an extended AZ that are similar to plants with ectopic expression of *IDA*, which suggests that either IDA might be excessively expressed or the HAE/HSL2 receptor complex might be activated in *nev/evr* flowers (Leslie *et al.*, 2010).

### ***DELAYED ABSCISSION 1, 2 and 3***

Mutants of the *delayed abscission 1* (*dab1*) 2 and 3 gene were isolated by screening for T-DNA lines with phenotype of delayed floral organ abscission (Patterson and Bleecker, 2004). All of the three *dab* mutants showed a normal response to ethylene treatment, suggesting that *DAB1*, 2 and 3 are act through an ethylene-independent-signalling pathway (Patterson and Bleecker, 2004).

### ***ACTIN-RELATED PROTEIN 7***

*ARP7* (*ACTIN-RELATED PROTEIN 7*) is an essential actin-related protein required for normal embryogenesis, plant architecture and floral

organ abscission in *Arabidopsis* (Kandasamy, *et al.*, 2005b). It is a novel and highly divergent member of the *Arabidopsis* ARP family unique to plants (McKinney *et al.*, 2002). *ARP7* has been localized to the nucleus (Kandasamy, *et al.*, 2003). Plants with the absence of *ARP7* exhibit stunted organs, reduced fertility and defects in flower opening, anther dehiscence and fruit growth, and a delay in floral organ abscission (Kandasamy, *et al.*, 2005b). RNAi plants with markedly reduced levels of *ARP7* showed a significant delay in the abscission of sepals, even though they developed normal AZs (Kandasamy, *et al.*, 2005b). The exogenous application of ethylene did not suppress the delayed floral organ abscission in *ARP7* RNAi plants, which suggests that *ARP7* is also involved in an ethylene-independent pathway controlling floral organ abscission in *Arabidopsis* (Kandasamy, *et al.*, 2005b).

### ***AGAMOUS-LIKE 15***

*AGAMOUS-LIKE 15 (AGL15)* is a member of MADS-box domain transcription factor family and constitutively expression of *AGL15* with 35S promoter courses delays embryonic development, flowering time, fruit maturation, senescence and abscission in *Arabidopsis* (Fernandez *et al.*, 2000; Harding *et al.*, 2003). 35S:*AGL15* plants showed an

acceleration in abscission when treated with ethylene, suggesting that *AGL15* is acting in an ethylene-independent-signalling pathway and plays a role in the inhibition of floral organ shedding after AZ differentiation (Fernandez *et al.*, 2000).

### **AUXIN**

Auxin (IAA) is an essential plant hormone that plays an important role in virtually every aspect of plant growth and development. IAA biosynthesis has been detected in dividing and growing tissues such as shoots and roots (Palme and Gälweiler, 1999). It is widely accepted that a balance between different hormones regulates the abscission process and that ethylene-independent pathway exists (Roberts *et al.*, 2002). For example, auxin is believed to act as a “brake” whilst ethylene acts as an “accelerator” in regulating the timing of abscission (Sexton and Roberts, 1982; Roberts, *et al.*, 2002; Dolan, 1997). It was suggested auxin repress abscission by preventing AZ from responding to ethylene (Meir *et al.*, 2006) and affecting some abscission-related genes (Hong *et al.*, 2000; dal Degan *et al.*, 2001). Several genes encoding auxin response factors (ARF) family have been reported to play a role in regulating abscission.

The genes *ARF1*, *ARF2*, *NONPHOTOTROPIC HYPOCOTYL4 (NPH4)*, and *ARF19* belong to an *Arabidopsis AUXIN RESPONSE FACTOR (ARF)* family. It has been demonstrated that these 4 transcription factors are functional in promoting senescence and floral organ shedding (Ellis *et al.*, 2005; Okushima *et al.*, 2005). The mutant *arf2* shows a delay both in senescence and floral organ abscission and *arf1 arf2* double mutants and *arf2 nph4 arf19* triple mutants also exhibit a substantial delay in abscission compared to the *arf2* single mutants (Ellis *et al.*, 2005). When changing auxin gradients in the floral organs, 4 genes, *ARF1*, *ARF2*, *ARF19* and *NPH4* could play an important role in promoting abscission by regulating ethylene biosynthesis (Ellis *et al.*, 2005).

### **1.1.3 Regulation of cell separation and shedding of organs.**

Once abscission is initiated, different enzymes start to modify the walls of AZ cells and dissolve the middle lamella (Morre, 1968).

#### ***β-1,4-endo-glucanase***

The first enzyme published to contribute to cell wall loosening in the AZ was *β-1,4-endo-glucanase (EGase)* (Sexton and Roberts. 1982).

EGase family has been classified into three subfamilies:  $\alpha$ -EGases and  $\beta$ -EGases are associated with cell elongation, ripening and abscission, while  $\gamma$ -EGases are involved in cell elongation and cellulose biosynthesis in the plasma membrane (Libertini *et al.*, 2004). The EGase family enzymes are thought to loosen cell walls by releasing xyloglucan (Hayashi, 1989; Cosgrove, 2005). It was found that the activity of this enzyme increased almost ubiquitously in the AZ tissues during shedding. BEAN ABSCISSION-SPECIFIC CELLULASE (BAC) was the first AZ specific wall degrading enzyme cloned from *Phaseolus vulgaris* (Lewis and Varner, 1970; Tucker *et al.*, 1988). Using BAC sequence another EGase gene was isolated and shown to be expressed in the AZ of soybean (Kemmerer and Tucker, 1994), *S. nigra* (Taylor *et al.*, 1994) and tomato (Lashbrook *et al.*, 1994). It has been shown that the expression of tomato EGases genes *Cel1* and *Cel5* are increased, while *Cel6* is decreased during pedicel abscission (Lashbrook *et al.*, 1998). Single mutation of either *Cel1* or *Cel2* using an antisense RNA strategy resulted in an increase in pedicel breakstrength but did not prevent abscission and the fruit softening was not affected, which suggests that *Cel1* and *Cel2* are cooperative during abscission but redundant during fruit maturation (Lashbrook *et al.*, 1998; Brummel *et al.*, 1999). In *Arabidopsis* there are 25 putative

EGases but none of them has been proved to be specifically abscission-related (Roberts *et al.*, 2002).

### **Polygalacturonase**

Another enzyme, polygalacturonase (PG), whose activity was also found to increase during cell separation, was first detected in ripening fruit (Huber, 1983), and the first AZ-specific PG isolated was *TAPG1* in tomato (Kalaitzis *et al.*, 1995). Then, *TAPG2*, *TAPG4* and *TAPG5* were identified using *TAPG1* as a probe (Kalaitzis *et al.*, 1997; Hong and Tucker, 2000). In *Arabidopsis*, over 69 putative PG genes can be identified based on sequence homology (Gonzalez-Carranza, *et al.*, 2002). In order to identify the abscission-related PG, analysis of the gene expression in AZ cells is an ideal way, however the small number of cells in *Arabidopsis* AZs makes it hard to isolate RNA and protein. To solve this problem, Gonzalez-Carranza *et al.* (2002) used a closely related species *B. napus* (oilseed rape), which has a larger AZ to isolate a PG cDNA. This PG cDNA was used as a probe to identify corresponding genomic clones both in *B.napus* (*PGAZBRAN*) and in *Arabidopsis* (*POLYGALACTURONASE ABSCISSION ZONE A. THALIANA*, *PGAZAT*). Fusion of the 1476 bp of the promoter of

*PGAZAT* to GUS revealed expression of this reporter gene at the base of the cauline leaves, anther filaments, petals and sepals at the time of shedding (Gonzalez-Carranza *et al.*, 2002). Under two different conditions, the absence and presence of ethylene, the *PGAZAT* mutant plants showed a delay in floral organ abscission compared to the wild type, suggesting that *PGAZAT* promotes cell separation in abscission (Gonzalez-Carranza *et al.*, 2007). *PGAZAT* was re-characterized by Ogawa *et al.* (2009) as *ARABIDOPSIS DEHISCENCE ZONE POLYGALACTURONASE 2 (ADPG2)* as it played an important role in silique dehiscence as. *ADPG1*, *ADPG2* and *QUARTET2 (QRT2)* are three closed related endo-PGs in *Arabidopsis* and *QRT2* plays an important role in floral organ abscission (Ogawa *et al.*, 2009). Single mutation in *QRT2* results in a delay in abscission, double mutations in both *ADPG2 (PGAZAT)* and *QRT2* results in a delay slightly greater, suggesting a functional redundancy (Ogawa *et al.*, 2009).

### **Expansin**

Expansin has been shown to facilitate cell wall loosening during wall extension (Cosgrove, 2000; Belfield *et al.*, 2005). It has been shown by immunogold labeling strategy that expansin presents in all layers of the



cell wall and occasionally in Golgi-derived vesicles (Cosgrove *et al.*, 2002). Under ethylene treatment, the activity of expansin in AZ increases sevenfold exclusively compared to only a small change in non-AZ tissue in *Sambucus nigra* (Belfield *et al.*, 2005). An RT-PCR result using cDNA library constructed from ethylene-treated leaflet AZ cells in *Sambucus nigra* revealed four enriched expansin genes: *SniEXP1*, *SniEXP2*, *SniEXP3* and *SniEXP4*, which suggested that expansin was enriched in leaflet AZ cells (Belfield *et al.*, 2005). In addition, down-regulation of gene *AtEXP10* in *Arabidopsis* results a reduced frequency of complete breakage of flowers forcibly removed from inflorescence stem, while overexpression of *AtEXP10* results an increase, which suggests that expansin may play an important role in abscission (Cho and Gosgrove, 2000). However, there has been no report about any other single expansin mutants apart from *atexp10* that have a pronounced phenotype in abscission. The reason for this could be that there is genetic redundancy among the members in the *Arabidopsis* expansin family (Cosgrove *et al.*, 2002; Li *et al.*, 2003).

### **Arabinogalactan-protein**

Arabinogalactan-proteins (AGPs) are a family of heavily glycosylated proteins that are detected in plant cell walls (McNeil *et al.*, 1984). In

*Arabidopsis* root tissue, AGPs have been shown to potentially mediate interactions between cell wall and cortical array of microtubules, which regulates the direction of expansion of root hairs (Andeme-Onzighi, 2002). AGPs were also detected to be ectopically secreted in mutants with overexpression of *IDA* (Stenvik *et al.*, 2006). The function of AGPs is not clear but all the clues point to molecular interactions and cellular signalling on the cell surface (Showalter, 2001).

### **Pathogen-related proteins**

When a certain organ is shed, it provides a good site for the invasion of pathogens. It has been predicted that there are at least two types of AZ cell. One of them is responsible for secreting wall hydrolyzing enzymes which cause cell separation and the other is responsible for protection against pathogen attack (Roberts, 2000). The gene *SHINE 1* (*SHN1*) in *Arabidopsis* has been reported to encode an AP2/EREBP transcription factor and play an important role in the regulation of protection layer as ectopically expressing *SHN1* results in shiny bright green surfaces and increased drought tolerance (Aharoni *et al.*, 2004). It has been shown that pathogen-related proteins (PR protein) have been detected at the site of abscission (Coupe *et al.*, 1997; Aharoni *et al.*, 2004). In

*Arabidopsis*, a number of PR proteins, such as  $\beta$ -1,3-glucanases and jasmonic acid biosynthetic enzymes has been demonstrated to be upregulated specifically in the floral AZ (Kubigsteltig, *et al.*, 1999; Volko, *et al.*, 1998). PR proteins such as  $\beta$ -1,3-glucanases, chitinases, thaumatin-like proteins, PR4-like protein, metallothionein-like proteins and allergen-like protein were also detected in the AZs of bean, tomato and *Sambucus nigra* (del Campillo and Lewis, 1992; Coupe *et al.*, 1995; Harris *et al.*, 1997; Ruperti *et al.*, 1999).

## **1.2 The root hair development in *Arabidopsis thaliana***

In the study of this project, some of the phenotypes were observed in the mutants root hairs. These phenotypes gave us clues in understanding the process of floral organ abscission. Therefore part of research in this project was carried out in the mutants root hair development. An introduction on root hair development is given below.

### **1.2.1 *Arabidopsis* root hair**

In the study of this project, some of the phenotypes, such as swollen and shortened root hairs, were observed in the mutants. These

phenotypes gave us clues to understand the process of floral organ abscission, as interestingly, both of the phenotypes, swollen root hairs and abnormal abscission are correlated with changing of the arabinogalactan protein (AGP) (Stenvik et al., 2006; Andeme-Onzighi et al., 2002). Therefore part of research in this project was carried out in the mutants root hair development. An introduction on root hair development is given below.

### **1.2.2 The development of *Arabidopsis* root hair**

An *Arabidopsis* root hair in an active tip-growth process has a polarized organization. The structures from the outside of the hemispherical apex are: an  $\alpha$ -layer of cellulose cell wall and a dense cytoplasm filled with secretory vesicles (Carol and Dolan, 2002) containing specific cell wall components (Sherrier and VandenBosch, 1994). Carol and Dolan (2002) separated root hair development into four phases: (1) the specification of hair-producing cells; (2) the initiation of root hair growth; (3) tip growth and elongation; and (4) cessation of mature root hair growth.

### **1.2.2.1 The specification of hair-producing cells**

The epidermal cells that are going to develop as hair-producing cells are predetermined. In *Arabidopsis* and other Brassicaceae family plant species, epidermal cells located over the intercellular space between underlying cortical cells, will develop into hair-producing cells (Cormack, 1935; Bunning, 1951; Dolan *et al.*, 1994; Galway *et al.*, 1994), which are called trichoblasts whereas epidermal cells located over single cortical cells develop into non-hair-producing cells, are called atrichoblasts (Dolan *et al.* 1994).

### **1.2.2.2 The initiation of root hair growth**

The gene *ROOT HAIR DEFECTIVE 6 (RHD6)* has been shown to be crucial for the selection of initiation site of root hair in *Arabidopsis thaliana* (Masucci and Schiefelbein, 1994; Masucci and Schiefelbein, 1996). Mutants without the presence of RHD6 show a reduction in the amount of root hairs, an overall basal shift in the root hair initiation site and a frequency in tritroblast with multiple root hairs (Masucci and Schiefelbein, 1994). Similar phenotypes were observed in auxin and ethylene resistant mutants *auxin resistant 2 (axr2)* and *ethylene receptor 1 (etr1)* (Masucci and Schiefelbein, 1994). The effects caused

by auxin and ethylene in root hair development have been discussed in detail by Wilson *et al.*, 1990; Kieber *et al.*, 1993; Leyser *et al.*, 1996 and Rahman, 2002.

After the determination of the root hair initiation site, a small bulge starts to develop, which was shown to require acidification of the cell wall (Bibikova *et al.* 1998). During this process, gene *RHD1* (or *ROOT EPIDERMAL BULGER1-1 (REB1-1)*) (Schiefelbein and Somerville, 1990; Andeme-Onzighi *et al.*, 2002) and *TIP GROWTH DEFECTIVE 1 (TIP1)* (Ryan *et al.*, 1998) have been shown to be responsible for the cell wall loosening. Mutants *rhdl (reb1-1)* produce root hairs with swollen bases but the total length was not affected (Schiefelbein and Somenrille, 1990). Compared to the wild type, in the *reb1-1* mutant root microtubules were found to be disrupted and arabinogalactan-proteins (AGPs) were not detected, which suggests that AGPs are required for cell wall expansion and orienting cortical microtubules (Andeme-Onzighi *et al.*, 2002). The mutant *tip1* displays a decrease in the length of root hairs (Schiefelbein *et al.*, 1993). In some *tip1* mutants, several short wide root hairs with wide bases have been observed (Ryan *et al.*, 1998).

The amount of root hairs per tritroblast has been shown to be controlled by *TIP1*, *TIP1*, *COW1* (*CAN OF WORMS*), *SCN1* (*SUPERCENTIPEDE*), *BST1*(*BRISTLED*), *CEN1* (*CENTIPEDE*), *CEN2* and *CEN3* and mutation of these genes result in a proportion of multiple root hairs emerging from a single initiation site (Grierson *et al.*, 1997; Ryan *et al.*, 1998; Parker *et al.*, 2000).

### **1.2.2.3 Tip growth and elongation**

#### **Transition to tip growth**

After the development of the bulge, the transition to tip growth and elongation of root hair starts. During the elongation process, a calcium gradient has been detected to accumulate in the tip of the root hair (Schiefelbein *et al.*, 1992; Wymer *et al.*, 1997). Extracellular calcium gradient has been shown to be required in *Arabidopsis* root hair growth (Schiefelbein *et al.* 1992). Inhibiting the calcium channel transport prevents root hair growth (Schiefelbein *et al.* 1992). A mutation in the *RHD2* gene results in a root hair bulging site but no elongation takes place (Schiefelbein and Somerville, 1990) and tip-accumulated calcium gradient was not detected in *rhd2* mutants, which supports that hypothesis that the calcium gradient is required for root hair development (Wymer *et al.*, 1997).

*SHAVEN 3 (SHV3)* was shown to act downstream of *RHD2* and *shv3* mutants do not elongate in the root hairs (Parker *et al.*, 2000). Mutations in *SHV1* and *SHV2* genes result in a similar phenotype, and SHV genes are shown to play an important role in establishing the tip growth of root hair (Parker *et al.*, 2000).

The gene *TINY ROOT HAIR 1 (TRH1)* has been shown to encode a K<sup>+</sup> transporter and mutant without *TRH1* fails to transfer to a tip growth (Rigas *et al.*, 2001). Disruption of the K<sup>+</sup> channel results in the inhibition of root hair growth transiently (Lew, 1991) but the mechanism of how K<sup>+</sup> channel affects root hair development is not yet clear (Rachel and Dolan, 2002).

The *kojak (kjk)* mutant forms a bulging in trichoblasts but fails to transfer to tip growth, and instead the bulging continues to expand until it bursts (Favery *et al.*, 2001). *KJK* was predicted to act specifically in root hairs and to be involved in the synthesis of cell wall (Rachel and Dolan, 2002). Cellulose synthesis has been shown to be required for tip growth and a similar phenotype to that seen in *kjk* was detected in the plants treated with cellulose synthesis inhibitor (Favery *et al.*, 2001).



### **Tip growth and Elongation**

Under normal growth conditions, *Arabidopsis* root hairs can achieve a length of up to 800µm and a diameter of 11µm (Galway *et al.* 1997). To achieve this morphology a plant must control the extension and orientation. It is believed that extension is driven by turgor pressure, which is isotropic, therefore for the orientation purpose the cell wall is considered to be the major determinant of morphogenesis (Roberts, 2001). For the tip growth, the cell wall of the root hair must be restructured at the apex and expansins have been shown to play an important role in loosening the cell wall polymers (Baluska *et al.*, 2000; Cosgrove, 2000).

The cytoskeleton plays an important role in root hair elongation. F-actin has been shown to be essential to maintain the localized growth of root hair cells (Bibikova *et al.*, 1999) and absence of F-actin results in root hair tip to be slightly deformed (Baluska *et al.*, 2000). Cytoskeleton microtubules (MTs) have been shown to play an important role in the polar growth of the root hair (Bibikova *et al.*, 1999). MTs were detected to be dynamic and parallel with the growth direction of root hair (Baluska *et al.*, 2000), Plant treated with the MT stabilizing drug Taxol

displays wavy root hairs and branches which suggest that MT is necessary for maintaining the calcium influx machinery at the tip of root hairs (Bibikova *et al.*, 1999). *ARMADILLO REPEAT KINESIN 1/ MORPHOGENESIS OF ROOT HAIR 2 (ARK1/MRH2)* has been shown to control the cellular organization of MTs (Jones *et al.*, 2006; Yang *et al.*, 2007; Sakai *et al.*, 2008). *MRH2* was predicted to be involved in RHO-RELATED PROTEIN (ROP2) GTPase controlled pathway, which coordinates actin filaments and MT in the process of polarized growth of root hairs (Yang *et al.*, 2007). In the *Arabidopsis* mutant *reb1-1*, swollen root hairs are accompanied by an absence of AGP and disruption of cortical MTs, which suggests that the interaction between cell wall and cortical MTs may be mediated by AGPs (Andeme-onzighi *et al.*, 2002).

A number of genes have been shown to affect the length of the root hair and absence of these genes results in shorter root hairs comparing to wild type. Mutation of *RHD3* causes short and wavy root hairs which suggests that *RHD3* is involved in tip growth (Galway *et al.*, 1997). Further analysis revealed that *RHD3* is essential for the cell wall biosynthesis and actin organization (Hu *et al.*, 2003). A similar phenotype was observed in *rhd4* mutants (Galway *et al.*, 1999). *RHD4*

has been shown to encode a Phosphatidylinositol-4-Phosphate Phosphatase which is necessary for *Arabidopsis* root hair development (Thole *et al.*, 2008). Mutants *bristled 1 (bst1)* *centipede 1 (cen1)*, *cen2*, *cen3*, *supercentipede 1 (scn1)*, *can of worms1 (cow1)* also have the similar phenotype (Grierson *et al.*, 1997; Ryan *et al.*, 1998; Galway *et al.*, 1997; Parker *et al.*, 2000). Parker *et al.* (2000) suggested that these genes control the shape of root hairs and *SCN1*, *BST1*, *CEN2*, and *CEN3* determine the amount of root hairs emerging from each single trichoblast (Parker *et al.*, 2000).

### **1.3 Aims and objective of the project.**

Previous microarray analysis within our group identified six genes in *Arabidopsis* that are potentially abscission related. The aim of this Ph.D project was to characterize their role during floral organ abscission. The initial objective was to undertake a detailed expression analysis using reporter genes. Based on the results generated from the expression analysis, further characterization then focused on one of the six genes, *At1g64405 (G2)*. Gene manipulation strategies were applied to generate down-regulation and over-expression lines of *G2*.

The phenotypes of the transgenic lines were then characterized to analyze the potential role that G2 might play during the abscission process. Furthermore, bioinformatics analysis was applied to study G2 protein structure in order to predict the potential function of G2.

Another aim of this project was to undertake analysis of the G2 promoter to probe the regulation of expression of abscission-related genes during the processes of organ shedding. The objective was to identify a potential abscission- related transcription factor binding motif and then analyze the motif. The approach adopted was to fuse the motif with a minimal promoter and GUS reporter gene and to determine spatial and temporal patterns of reporter gene expression.

## **CHAPTER 2**

### **Materials and methods**

#### **2.1 Materials**

##### **2.1.1 Plant materials and growth conditions**

Plants of Columbia-0 *Arabidopsis* and all the mutants were grown in plastic pots containing Levington M3 compost and Vermiculite in 3:1 ratio mix supplemented with 0.2 g/L of Intercept 70 WG (Sotts, Monro South) under greenhouse conditions with 16 h of light and 8 h dark at  $23\text{ }^{\circ}\text{C} \pm 1\text{ }^{\circ}\text{C}$ .

## 2.1.2 Bacterial strains and Plasmid vectors

***E. coli* DH5α:** Genotype: *supE44*, *hsdR17*, *recA1*, *endA1*, *gryA96*, *thi-1*, *relA1* (Hanahan, 1983).

***Agrobacterium tumefaciens* C58:**

It consists of a circular chromosome, a linear chromosome, and two plasmids (Wood, *et al.*, 2001).

**pDONR<sup>TM</sup>221:** A GATEWAY<sup>TM</sup> series vector used to make an entry clone. The pDONR<sup>TM</sup>221 vector has a pUC origin for high plasmid yields and universal M13 sequencing sites for ease of use.

**pGWB8:** A GATEWAY<sup>TM</sup> series vector. Contains 35S promoter, C-6 × His, Kanamycin and hygromycin resistant genes. (Nakagawa, Shimane University, Japan.)

**pGWB4:** A GATEWAY<sup>TM</sup> series vector. Contains C-6 × His, Kanamycin and hygromycin resistant genes. (Nakagawa, Shimane University, Japan.)

**PK7GW1WG2:** A GATEWAY™ series vector used to generate a RNAi line of gene At1g64405 contains spectinomycin and kanamycin resistant genes. (Karimi *et al.*, 2005)

**MOG257:** A pMOG series vector contains a GUS gene and a 257bp minimal promoter before GUS.

### **2.1.3 Primers**

The following primers in table 2.1 were used in this project.

All primer sequences are given 5' to 3'.

	Primer	Sequence	Tm °C	Functions
1	G2 Forward	GGGAATTGATGGGCAATTGCATGG	70.42	To amplify the <i>G2</i> cDNA fragments
	G2 Reverse	CATTTCCTGGACTTCTGGACACTC	62.03	
2	G2_Promoter Forward	GGCGAAGTTTCATACCGTTGACTTG	65.51	Used in combination with LBb1 primer to confirm the T-DNA insertion in KO lines
	G2_Promoter Reverse	CTCCATGCAATTGCCCATCAATTCCC	71.95	
3	G2AttB_Forward	GGGGACAAGTTTGTACAAAAAGCAGGCTTC	70.42	To amplify the <i>G2</i> cDNA fragments with AttB Sites
	G2AttB_Reverse	ATGGGCAATTGCATGGAGA		
4	IDA Forward	GGGGACCACTTTGTACAAGAAAGCTGGGTCT	62.03	To amplify the <i>IDA</i> cDNA fragments
	IDA Reverse	TATCTATCCATTTCCTGG		
5	IDA Forward	TCGCGGCGAGTAGTTCTTGTGT	58.61	To confirm of the T-DNA insertion
	IDA Reverse	GCAGAAGGAGGAATGGGAACGCC	59.81	
6	LBb1	GCGTGGACCGCTTGCTGCAACT	71.43	To confirm the successful insertion of the fragments into the
7	M13 Forward	GTT TTC CCA GTC ACG ACG	62.34	To confirm the successful transformation of <i>G2</i> fragment into pK7GIWG2 destination vector
	M13 Reverse	CAG GAA ACA GCT ATG ACC	56.16	
8	PK7 Reverse	CAT ACC AAC AGG GTG CCA CCT	68.35	CAP-BINDING PROTEIN used as House-Keeping gene in RT-PCR
	HK-CBP Forward	CGTGAAGCGATGGCTTCTTTGTTC	71.62	
9	HK-cbp Reverse	CTCCTCTTCATGGCCATTTGTC	70.58	Forward primer selected in CaMV35S promoter
	35S Forward	AAGGAAGTTCATTTTCAATTTG	56.33	
10	GUS_Sequence	TCACGGGTTGGGGTTTCTAC	66.21	To confirm the GUS sequence
	GFP_Sequence	TGGCGATGGCCCTGTCCTTT	58.32	To confirm the GFP sequence
11	MOG257Forward	CTG AAG GCG GGA AAC GAC	66.2	To confirm the successful transformation of <i>G2</i> fragment into MOG257 destination vector
12	MotifRepeat 1 Forward	GCTAAAGCTTAATATACATTCTCGAGTAGC	62.62	These primers are used as single strand DNA sequences for annealing to produce motif AATATACATT with 1, 2 and 3 repeats.
	MotifRepeat 1 Reverse	GCTACTCGAGAATGTATATTAAGCTTTAGC	63.62	
13	MotifRepeat 2 Forward	GCTAAAGCTTAATATACATTAATATACATTC	66.46	
	MotifRepeat 2 Reverse	TCGAGTAGC	66.46	
14	MotifRepeat 3 Forward	GCTACTCGAGAATGTATATTAATGTATATTA	68.22	
	MotifRepeat 3 Reverse	ATATACATTCTCGAGTAGC	68.22	

**Table 2.1:** Primers used in this project.



## **2.2. Methods**

### **2.2.1 Growth and maintenance of bacterial strains**

The *E. coli* DH5 $\alpha$  and *Agrobacterium tumefaciens* C58 strains were cultured and maintained in standard Luria-Bertani (LB) medium. The *E. coli* DH5 $\alpha$  was grown at 37 °C overnight and the *Agrobacterium tumefaciens* C58 was grown at 29 °C for 48 h. The strain was stored at -70 °C as described by Sambrook *et al.* (1989). Cells containing plasmids that conferred kanamycin, spectinomycin, hygromycin and rifampicin were grown in LB broth plus kanamycin, spectinomycin, hygromycin or rifampicin at 50  $\mu$ g/ml, 50  $\mu$ g/ml, 50 $\mu$ g/ml and 35 $\mu$ g/ml, respectively.

### **2.2.2 Growing *Arabidopsis* materials on Murashige and Skoog basal salt mixture (MS) medium**

The sterilization of *Arabidopsis* seed was carried out in a sterile flow hood. Seeds were put in a 1.5 ml Eppendorf tube, and washed with 50% (v/v) bleach. After at least 5 min the seeds were then washed twice with 0.01% (v/v) Triton-X100, and then the seeds were re-suspended in 70% (v/v) ethanol for 1 min followed by washing the seeds with sterile distilled water 3 times. Finally the seeds were poured

onto sterile 3MM Whatman paper to air dry in a flow hood. The dry seeds were placed on Petri plates containing Murashige and Skoog basal salt mixture (MS) medium, with pH 5.9, and 0.8% (w/v) agar. The plates with the seeds were placed in refrigerator at 4 °C for 48 h to promote even germination, after which the plates were transferred to a growth room at a temperature of 23°C  $\pm$  1°C under 16 h light and 8 h dark.

### **2.2.3 *Arabidopsis* crossing**

*Arabidopsis* crossing was performed under a stereo microscope. All the siliques, young flower buds and flowers with petals were removed by using a tweezer until around 4 large buds without white petals visible remained on each inflorescence. Then the sepals, petals and anthers were removed without damaging the pistils. A fully opened flower from a donor plant was used to apply pollen to the stigma. Different genotype crosses were performed after sterilization of the tweezers using 70% (v/v) ethanol.

### **2.2.4 GUS staining assay**

Material from different stages of development and tissues including seedlings, roots, cauline leaves, flowers, young siliques and mature siliques were placed in GUS substrate (contains 0.2M phosphate buffer pH 7.0, 1 mM X-Gluc, 0.5M EDTA and 0.1% (v/v) X-100 Triton) and incubated at 37 °C for 2 h. Then the material was put in 100% (v/v) ethanol or Chloral Hydrate solution (contains 28% (w/v) Chloral Hydrate and 33% (v/v) Glycerol 100%.) to remove chlorophyll.

### **2.2.5 Genomic DNA isolation**

Genomic DNA was isolated from cauline leaf tissue using GenElute™ Plant Genomic DNA miniprep Kit (Sigma-Aldrich) according to the manufacturer's instructions. 100 mg of cauline leaf tissue was disrupted and ground in liquid nitrogen into a fine powder which was then transferred to a microcentrifuge tube. 350 µl of Lysis solution A and 50 µl Lysis solution B were then added and mixed by inverting the tubes several times. The mixture was then incubated at 65 °C for 10 min before 130 µl of precipitation solution was added. The mixture was then transferred into a filtration column followed by centrifugation at maximum speed (21,690 rcf). 500 µl wash solution was applied to the

column followed by centrifugation at maximum speed (21,690 rcf). For purification purposes, a silica-wash-elute procedure was performed using 100 µl of prewarmed elution solution (10 mM Tris, 1mM EDTA, pH 8.0) which was added followed by centrifugation at maximum speed (21,690 rcf). The resulting Purified DNA was used for PCR.

### **2.2.6 Polymerase Chain Reaction (PCR)**

The Polymerase Chain Reaction (PCR) was performed using MangoTaq™ DNA polymerase from Bioline™ according to the manufacturer's instructions. Unless otherwise stated the reaction was performed in 25 µl reaction volume containing 0.5 units of MangoTaq™ DNA polymerase, 100 ng of DNA template, 1 × PCR buffer, 0.2mM of dNTP, 1.5mM of MgCl<sub>2</sub> and 50ng of specific primers respectively. PCR reactions were performed in an Eppendorf thermocycler. The standard programme commenced with 3 min incubation at 94 °C. The reaction was then performed for 30 – 35 cycles with each cycle being 30 seconds at 94°C to denature the DNA, 30 seconds at the annealing temperature and a certain duration

(depending on the length of products) at 72°C for the extension. After the cycles the reaction was held at 72°C for 7 min and kept at 4°C. To obtain high fidelity PCR products, Phusion™ High-Fidelity DNA Polymerase from BioLabs was used to amplify the DNA following the manufacturer's instructions. Products of PCR were visualized on a 1% - 1.5% (w/v) agarose gel depending on the length of products.

### **2.2.7 RNA isolation and quantitative Reverse-Transcription PCR (qRT-PCR) Analysis**

Total RNA from flowers and young siliques was isolated using an RNeasy™ (QIAGEN) Kit according to the manufacturer's instructions. Plant tissue was frozen and liquid nitrogen and to ground a fine powder. 100 mg tissue powder was then disrupted with 450 µl buffer RLT (RNeasy Lysis Buffer contains guanidine thiocyanate) with 10 µl/ml β-Mercaptoethanol (β-ME). The mixture was then transferred to a QIAshredder spin column placed in a 2 ml collection tube following centrifugation for 2 min. The supernatant was transferred to a new 1.5 ml tube and 225 µl ethanol (96% - 100%) (v/v) was added and mixed quickly by pipetting. The mixture was then transferred into an RNeasy spin column placed in a 2 ml collection tube following a centrifugation

at max speed for 15 s. 700 µl of buffer RW1 (containing 2.5 – 10% of guanidine thiocyanate) was added followed by centrifugation at max speed for 15 s. The residue was then washed twice by 500 µl buffer RPE before dissolving in 40 µl RNase-free water.

The resulting total RNA was quantified with a Nanodrop ND-1000 Spectrophotometer. First-strand cDNA synthesis with SuperScript II reverse transcriptase (Invitrogen™) was performed in a total volume of 20ul with 4 µl of 5 X Buffer and 2 µl of 0.1M DTT, using 500ng of total RNA as template and incubated at 42 °C for 60 - 70 min. 1-2µg of RNA was run on 1% (w/v) agarose gel in 0.5 × TBE electrophoresis buffer at 90 V/cm in order to check the integrity of the RNA prior to RT-PCR analysis. Isolated RNA was kept in the -80 °C freezer. To analyze the specific primers, a semi-quantitative PCR was carried by using 3 µl of the cDNA as a template in a 25ul PCR reaction containing 10 × PCR Buffer 2.5ul, 0.75 mM MgCl<sub>2</sub> 2.5ul, 5mM/ul dNTP 1ul, 1.25 units of MangoTaq™ DNA Polymerase, 50 ng forward primer, and 50 ng reverse primer. HK-CBP primers were used as a control in the PCR to confirm that the quantity of RNA isolated was consistent. The product of PCR was visualized on a 1% (w/v) agarose gel.

The specific genes *G2* and *IDA* were analyzed by qPCR with *F-ACTIN* as the housekeeping gene. The qPCR reaction composed of 3 µl of first stand cDNA, 10.0 µl of Fast SYBR® Green Master Mix (2 ×) (Applied Biosystems), 2 µl of 10 pM forward and reverse primer, and sterilised water added to 20 µl. The qPCR was carried out in Duplicate. The standard control was made from 3 µl of each sample and then mixed together. 4 µl of the mixture was taken and added 36 µl of sterilised water to make a 10 times dilution. Then another 4 µl were taken from diluted sample ( $10^{-1}$ ) to a 36 µl of sterilised water to make 100 times dilution ( $10^{-2}$ ). The standard control was diluted until  $10^{-5}$  and base on which a standard curve was generated. The standard curve was generated in Duplicate. The qPCR was performed for 45 cycles with each cycle being 10 seconds at 94°C to denature the DNA, 50 seconds at the annealing temperature and 15 sec at 72°C for the extension.

### **2.2.8 *E. coli* DH5α Transformation with Plasmid DNA**

The constructs was transformed into *E. coli* DH5α using the Heat-shock method (Sambrook *et al.*, 1989). 100 – 200 ng plasmid in a 2 µl

solution was added to 50 µl competent cells *E. coli* DH5α. The solution was then kept on ice for 30 min before it was heated at 42 °C in a water bath for 45 seconds. Immediately 1 ml of LB medium was added to the cells and the solution was then incubated with shaking at 37 °C for 1 h. The cells were then plated onto LB medium with appropriate antibiotic and incubated at 37 °C overnight.

### **2.2.9 Purification of Plasmid DNA**

For small scale purification of plasmid DNA, NucleoSpin™ Plasmid was used following the manufacturer's instructions. For large scale purification, the following method was applied: a 15 ml overnight culture was pelleted by centrifugation at 5,000 rpm for 5 min and the supernatant was discarded. The pelleted cells were dissolved in 600µl solution I containing 25 mM Tris-HCL, pH 8.0, 50 mM EDTA, pH 8.0 and 1% (w/v) glucose followed by addition of 800 µl solution II, containing 0.2 M NaOH and 1% (w/v) SDS. The mixture was mixed by gently inverting the tubes 8 to 10 times, and then 600 ml solution III which contained 0.2 M glacial acetic acid and 0.2 M KAc was added. The tubes were gently inverted 8 to 10 times before they were



centrifuged for 10 min at max speed. The supernatant was then separated and an equal volume of isopropanol added for precipitation of plasmid DNA. The pellet was then washed in 75% (v/v) Ethanol and dissolved in sterile distilled water before it was sent to NanoDrop for quantity and quality testing. The plasmid solution was then kept at -20 °C in a freezer.

### **2.2.10 Gateway BP reaction and LR reaction**

The BP and LR reaction were performed following the instructions of the manufacturer (Invitrogen™). For BP reaction, primers with attB1.1 and attB2.1 sites were designed (Section 2.1.3) and used to amplify the whole cDNA of gene *at1g64405* in a PCR reaction using Phusion™ High-Fidelity DNA Polymerase. The PCR products were purified before they were transformed into Gateway™ entry vector pDONR221.

### **2.2.11 *Agrobacterium* Transformation with Plasmid DNA**

The construct was transformed into *Agrobacterium* cells C58 by electroporation, using a pulse at 2,500 V. 100 – 200 ng plasmid in a 2

µl solution was transformed into a 50 µl *Agrobacterium* C58 competent cells. Immediately 1ml of LB medium was added to the cells and the solution was then incubated without shaking at 28 °C for 3 - 5 h. The cells were then plated onto LB medium with appropriate antibiotic and incubated at 28 °C for two days.

### **2.2.12 Plant transformation**

The Floral Dip method (Clough and Bent, 1998) was used to transform *Arabidopsis* plants with *Agrobacterium*. The *Agrobacterium* containing the target construct was grown for about 18 h in 200 ml LB medium with appropriate antibiotic at 28 °C, until an OD of 1.0-1.2 was reached. The cells were then centrifuged at 3500 r.p.m. for 5 min and resuspended in 200ml of 5% (w/v) sucrose, 0.05% (v/v) silvet L77. The flowers were then dipped in the solution for a few seconds and left in a sealed plastic bag in a humid atmosphere. The plastic bag was opened after two days and the plants were left to mature and until siliques had desiccated and were ready for seed harvesting.

### **2.2.13 Preparation of glycerol stocks**

Bacterial glycerol stocks were prepared by inoculating 2 ml of media culture (containing the appropriate antibiotic) with a single bacterial colony and incubating at 37 °C with shaking until an OD<sub>600</sub> of 0.5 – 0.7 was reached. 0.85 ml culture solution was transferred to a sterile tube and mixed with 0.15 ml of 100% (v/v) sterile glycerol. The culture was quickly frozen in liquid N<sub>2</sub> and stored at -80 °C freezer.

### **2.2.14 Annealing of single strand DNA sequences**

1µg of each strand DNA was dissolved in 1.5 mM of MgCl<sub>2</sub> 20 µl and incubated at 72 °C in a PCR machine for 30 min, and then cooled down at room temperature before they were sent for Nanodrop analysis.

### **2.2.15 Digestion of DNA fragments and plasmids using restriction enzymes**

The purified annealed DNA fragments or plasmids were digested with appropriate restriction enzymes (Fermentas) with the buffers and conditions according to the manufacturer's instruction. The general DNA digestion reaction was performed for 2 - 3 h at the recommended temperature (normally 37 °C). The digested products were kept at -20°C

### **2.2.16 Dephosphorylation of 5' overhangs**

The 5'-terminal phosphate groups were removed using Calf intestinal alkaline phosphatase (CIAP) from Promega<sup>TM</sup>. The CIAP was added into 40µl of DNA at a final concentration 0.01u/µl. Then the reaction tubes were incubated at 37°C for 30 min before adding the same amount of CIAP and incubated at 37°C for an additional 30 min. 300µl CIAP stop buffer containing 10mM tris-HCL (pH 7.5), 1mM EDTA (pH 8.0), 200mM NaCl and 0.5% SDS was added to stop the reaction. The dephosphorylated DNA solution was purified as described in chapter 2.2.9.

### 2.2.17 Ligation of DNA fragments

The linearized vector (50 ng) was mixed with purified DNA fragment (amount following the equation) in ligase buffer containing 50 mM Tris-HCl pH 7.5, 5.0 mM MgCl<sub>2</sub>, 5.0 mM 1,4-dithiothreitol (DTT), 10 mM ATP and T4 DNA ligase as in the following table (Table 2.3).

Ligation reaction	Insert	Control
10 × Ligase buffer	1µl	1µl
10 × Ligase	1µl	1µl
Insert	From equation below	-
Vector	50ng	50ng
Water	To 10µl	To 10µl

**Table 2.3** Equation:  $w(\text{insert ng}) = [w(\text{vector ng}) \times \text{size (insert bp)} / \text{size (vector bp)}] \times 3$

The ligation mixture was directly transformed in *E. coli* DH5α by the heat-shock method (Sambrook *et al.*, 1989).

### 2.2.18 Staining *Arabidopsis* flowers with Synthetic chemical reagent β-D-glucosyl Yariv (β-GlcY)

2mg β-D-glucosyl Yariv (β-GlcY) (Biosupplies) was dissolved in 1ml 0.15M NaCl. The tissue was incubated in the solution for 1 hour at room temperature and then washed in water for 3 times.

## 2.2.19 Immunolocalisation

5-day-old seedlings of 35SG2, *RNAiG2* and wild type were fixed by incubating in Thaw Fixative (BioMed) under vacuum for 1 hour. After the fixation, all the processes were performed by using an *In situ* pro liquid handling robot. Samples were washed by 6 × 12 min in PBS, and 3 × 12 min in Water in room temperature and 1 × 12 min at 37 °C. Samples were then treated by 0.3% - 1.0% Drieslase (Sigma) in MTSB (microtubule – stabilising buffer containing 50mM pipes, 5mM EGTA, 5mM MgSO<sub>4</sub> with pH 6.9 -7.0) for 60 min following washing in PBS for 10 × 12 min. Permeabilisation was performed by incubating the samples in 2 × PBS with 20% DMSO and 2% NP -40 for 1 hour. Samples were then washed for 10 × 12 min in PBS before the blocking process, which was performed by incubating the samples in 2% BSA at 37 °C for 1 hour. Antibody Antitubulin (Abnova™) was used for the primary antibody. The samples were incubated in blocking solution at 37 °C for 4 – 5 hours following washing in PBS for 10 × 12 min. Antibody Anti-rabbit IgG (Abnova™) was used as the secondary antibody. The samples were incubated in blocking solution at 37 °C for 4 – 5 hours following washing in PBS for 10 × 12 min. After the above treatments,

## Chapter 3

# Expression and bioinformatic analysis

### 3.1 Introduction

*POLYGALACTURONASE ABSCISSION ZONE A. THALIANA* (*PGAZAT*) has been shown to be expressed specifically in AZ cells (González-Carranza *et al.*, 2003; Ogawa *et al.*, 2009). In a previous project in the lab, the promoter of *PGAZAT* was fused to the Green Fluorescent Protein (GFP) reporter gene (González-Carranza *et al.*, unpublished data). Approximately 30,000 separating cells expressing GFP were collected and used to provide mRNA for the generation of an AZ cDNA library (Figure 3.1). By labeling the cDNA library and hybridizing probes to an Arabidopsis oligo array, a specific profile of AZ

transcripts was generated. Fifty most highly expressed genes were selected and a functional characterization determined (Figure 3.1). Six of these genes, *At3g56350* (G1), *At1g64405* (G2), *At2g23630* (G3), *At3g53040* (G4), *At2g44010* (G5) and *At5g50540* (G6) were identified of particular interest on the basis of their high expression in the AZ and their putative functions, which will be discussed in detail below. The promoters of the six genes were fused to GUS or GFP in order to analyze their spatial and temporal patterns of expression. Reporter gene expression showed that all of the six genes were expressed in the AZ at the time of floral organ shedding (Shahid, unpublished data not shown).



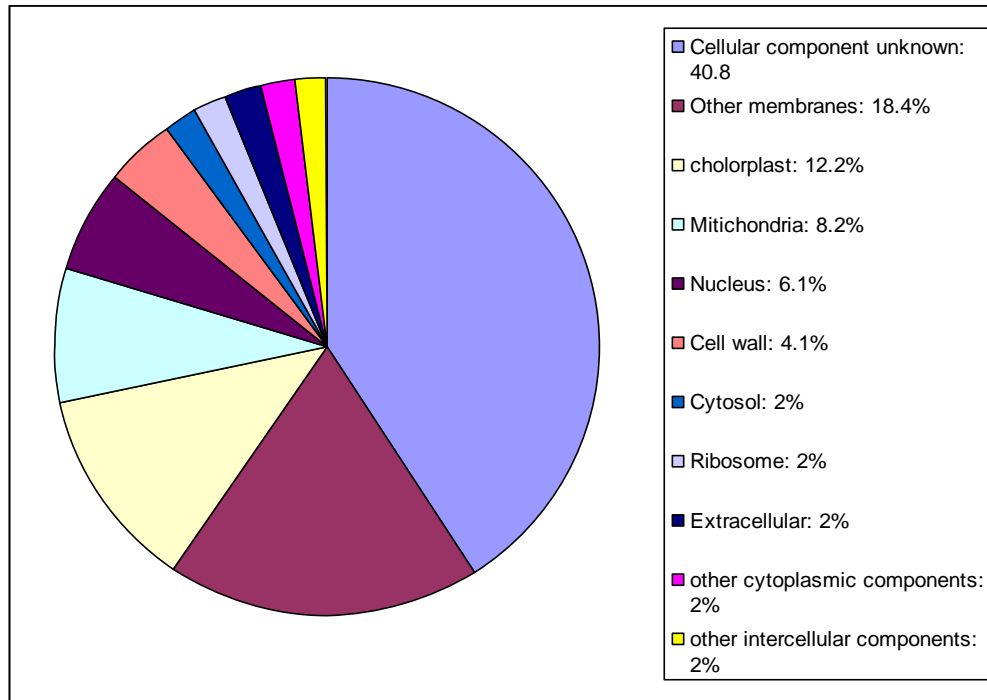


**Figure 3.1:** Functional categorization of the fifty most highly expressed genes which were selected from a cDNA library generated from the AZ Micro array data (González-Carranza *et al.*, unpublished data).

Gene Name	Locus	Putative function	Expressed in	Expression Value
<i>G1</i>	AT3G56350	Superoxide dismutase activity	Pollen, Seed	20410.4
<i>G2</i>	AT1G64405	Unknown	carpel, collective leaf structure, hypocotyl, pedicel, petal, plant embryo, pollen, root, sepal	3952.9
<i>G3</i>	AT2G23630	pectinesterase activity	hypocotyl, root, shoot apex	319.4
<i>G4</i>	AT3G53040	late embryogenesis abundant protein activity	Seed	5268.4
<i>G5</i>	AT2G44010	Unknown	Root	3024.9
<i>G6</i>	AT5G50540	Unknown	Pollen tube cell	574.8

**Table 3.1:** The expression information and putative functions of the six genes selected from the micro array data.

### ***At3g56350 (G1)***

Gene *At3g56350* encodes a cDNA of 935 bp. The protein data show that it contains a Mn Superoxide dismutases (SODs) domain. The functions of SODs domain proteins are usually to destroy the radicals that are normally produced within cells and are toxic to biological

systems (Bannister et al., 1987). *G1* belongs to a large family and WU-BLAST result shows that it shares 72% conservative region with another gene ***At3g10920*** which also contains a Mn Superoxide dismutases domain.

*G1* was selected as the micro array data showed a high level of expression (Table 3.1). Fusion of 884 bp of the promoter of *G1* to GUS revealed expression of this reporter gene at the base of the floral organs at the time of shedding (Figure 3.2).

#### ***At1g64405 (G2)***

The putative function of gene *At1g6440* (*G2*) is unknown. WU-BLAST result shows that it is a unique gene within the *Arabidopsis thaliana* genome. Searching of *G2* in Genevestigator\_V3 (<https://www.genevestigator.ethz.ch>) showed a significant high level of expression in the AZ, medium level of expression in the hypocotyl, radicle, carpel, pollen, lateral root, root tip and root hairs.

*G2* was selected of interest for the reason that microarray data showed a significantly high level of expression (Table 3.1). Fusion of 1865 bp of the promoter of *At1g64405* to *GUS* showed a strong expression

covering the whole of the AZ of floral organs that spread to adjacent non-separating tissues (Figure 3.2), and fusion of this promoter to *GFP* revealed specific expression in the AZ (figure 3.4, 3.6).

### ***At2g23630 (G3)***

G3 was selected as it was predicted to encode a putative pectinesterase which could potentially function in controlling oxidoreductase activity (Visser and Voragen, 1996). Pectinesterase is a ubiquitous cell-wall-associated enzyme that facilitates plant cell wall modification and subsequent breakdown (Deuel *et al.*, 1958) and cell wall degradation is well documented to take place during abscission.

Fusion of 1877 bp of the promoter of *At2g23630* to *GUS* showed that the reporter expression commenced at the base of the floral organs at the time of shedding (Figure 3.2).

### ***At3g53040 (G4)***

Gene *At3g53040* encodes a putative late embryogenesis abundant (LEA) protein. It belongs to a large LEA family which is expressed in late embryogenesis in higher plant seed embryos and under conditions of dehydration stress (White *et al.*, 1995). Plants endure different

stresses during organ shedding, therefore this gene was hypothesised to be of interest as it could potentially play a role in the stress response during abscission.

When 1655 bp of the promoter of *At3g53040* was fused to *GUS*, the reporter gene showed similar expression as *At3g56350* and *At2g23630* within the AZ area. The expression of *G4:GUS* was observed at the base of the floral organs (Figure 3.2).

### ***At2g44010 (G5)***

The function of gene *At2g44010* is unknown. WU-BLAST shows that *G5* shares 60% nucleotide homology with *At3g59880* however this gene was not identified from the micro-array data as differentially expressed (Gonzalez unpublished data).

*G5* was selected of interest as the micro array data showed a high level of expression. A region of 1303 bp of the promoter of *At2g44040* was fused to *GUS* and the reporter gene was showed to be expressed at the base of the floral organs (Figure 3.2).

### ***At5g50540 (G6)***

The function of the gene *At5g50540* is unknown.

Fusion of 1407 bp of the promoter of *At5g50540* to *GUS* showed the expression of the reporter gene at the base of the floral organs (Figure 3.2).

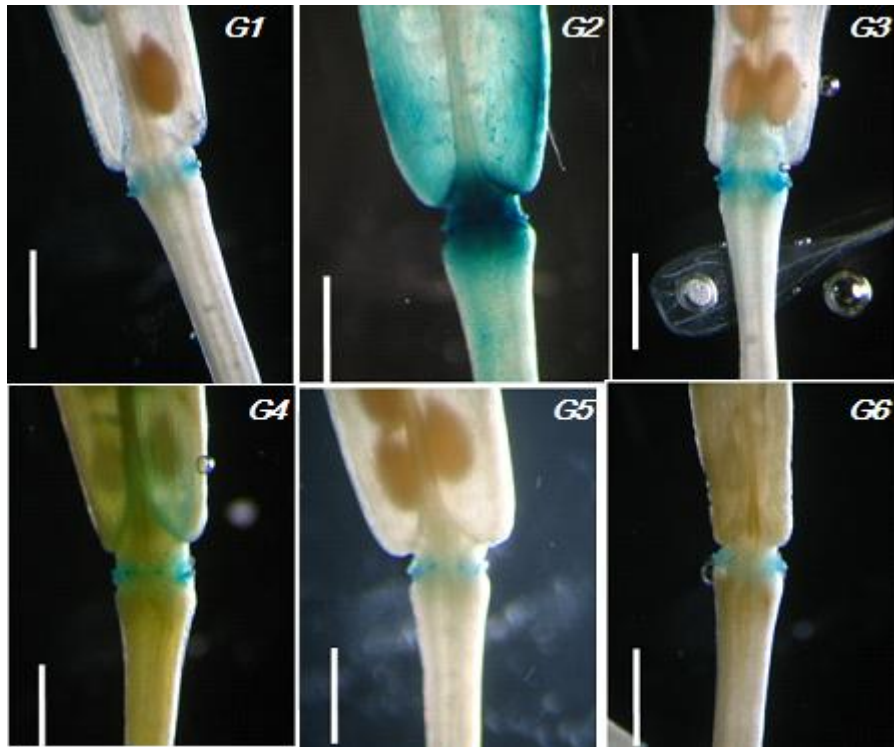


**Figure 3.2:** *G1<sub>Prom::GUS</sub>*, *G2<sub>Prom::GUS</sub>*, *G3<sub>Prom::GUS</sub>*, *G4<sub>Prom::GUS</sub>*, *G5<sub>Prom::GUS</sub>* and *G6<sub>Prom::GUS</sub>* expression in the abscission zone of the flowers at position 7 - 10. The constructs were built by fusing the promoters of the 6 genes to *GUS* (Dr Shahid, unpublished data).

Another strategy carried out at the start of this project was to analyze expression in putative knockout lines and analyze their phenotypes. T-DNA insertion lines into gene *G1*, *G2*, *G3* and *G4* had been identified previously (Shahid 2007 unpublished). RNA was extracted from young siliques and flowers of putative Knockout lines and the wild type. Primers were designed to amplify the cDNA for the 4 genes. From the RT-PCR results, no PCR amplification was observed from the T DNA insertion lines into *G1*, *G3* and *G4* (Figure 3.3a) compared to the clear band in the wild type control. *G2* expression was observed in both T DNA insertion line and wild type (see also chapter 4), indicating that *G2* had not been silenced in this putative knockout. (Fig. 3.3a, Fig. 3.3b).

**Figure 3.3a**

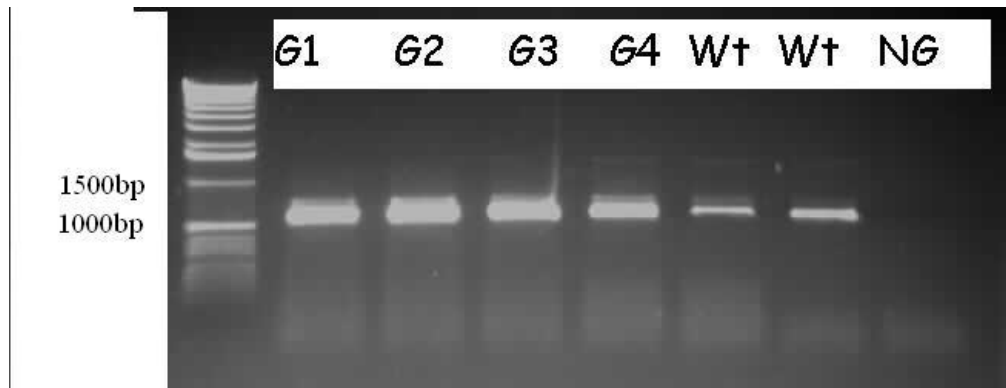


**Figure 3.3b**

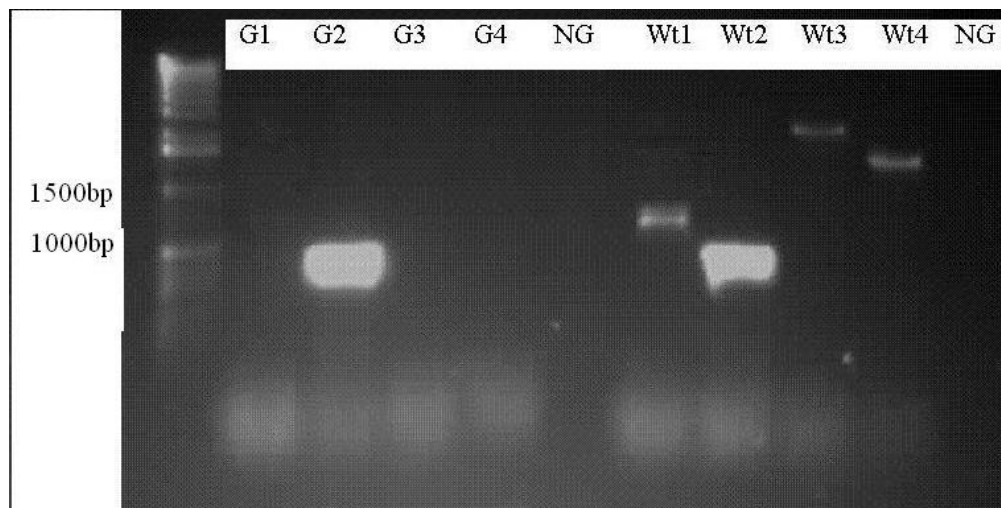


**Figure 3.3:** RT-PCR analysis to identify knockouts of the genes *At3g56350*, *At1g64405*, *At2g23630* and *At3g53040* (marked as G1, G2, G3 and G4). Fig. 3.3a shows the result of a control that all the cDNA was amplified using CAP-BINDING PROTEIN-primers (CBP) (Table 1.1). Fig. 3.3b shows that there was no expression in G1, G3, and G4 with specific cDNA primers compared to expression in the wild type. However, expression in the G2 insertion line was indistinguishable from wild type demonstrating that it is not a functional knockout.



Further analysis was then carried out to characterize the phenotype of KO lines of *G1*, *G3* and *G4*, however no differences in the abscission process were observed compared to the wild type plants under the growth conditions employed in this study. While the generation of KO lines of *G2*, *G5* and *G6*, the expression analysis was repeated on the *Prom::GUS* lines of *G1* – *G6* at the beginning of this project, however the *GUS* signal of *G1:GUS*, *G3:GUS*, *G5:GUS* and *G6:GUS* was not observed, which was not consistent with former results of our group. During the expression analysis, *G2* showed an interesting expression pattern, including highly AZ specific expression, expression in lateral root emergence sites where cell separation events occur - which will be described in the following chapters – therefore further study of this project was then focusing on the characterization of *G2*.

The transcript of *G2* is 357 bp in length and contains an ORF that is predicted to encode a polypeptide of 118 amino acids. *G2* was considered to be a unique gene as the WU-BLAST (<http://www.Arabidopsis.org/wublast/index2.jsp>) search showed that it did not share close homology with any other gene within the *Arabidopsis* genome. A microarray performed by treating IAA inhibitor in 10 day old *Arabidopsis* root tissue suggested that *G2* was up

regulated by IAA

(<http://affymetrix.arabidopsis.info/narrays/experimentpage.pl?experimentid=186>). *In silico* analysis using online tool Genevestigator\_V3 showed additional evidence that G2 was expressed specifically in the AZ (Hruz *et al.*, 2008) (<http://www.genevestigator.com/>).

### **3.2 Expression analysis of G2 (*At1g64405*)**

RT-PCR analysis showed that G2 was highly expressed in AZ tissue when cell separation was taking place (Chapter 3). It was believed that G2 was a potential abscission-related gene but this hypothesis was needed to be tested. The objective of this section was to characterize the expression pattern of G2. Crosses were carried out between G2 and different abscission-related mutants in order to confirm the hypothesis that G2 is abscission-related.

#### **3.2.1 Analysis of *G2:GUS/GFP* transgenic lines**

To investigate the expression pattern of G2 in Wild-Type background, the 1865 base pairs upstream of the translation start site of G2 were fused to the ORF of Green Fluorescent Protein (GFP) and beta-glucuronidase (GUS) (Shahid, unpublished data). Transformed *Arabidopsis* plants were analyzed for either *G2:GFP* or *G2:GUS*

reporter gene expression. The floral organs were inspected by using a time-course method to analyze the expression pattern of *G2*. *G2* showed strong and specific expression in the AZ cells as soon as the abscission process was taking place (Figure 3.4, 3.5). Only low levels of *G2:GUS* expression were detected in the AZs at the base of the floral organs from position 2 (position 1 corresponds to the first flower where petals are visible) to 6. From position 7 - 8, GUS expression dramatically increased as soon as the abscission process began. The accumulation of GUS was seen to spread towards non-AZ cells, which might be the consequence of GUS products spreading through the vascular tissue. The expression was maintained throughout the development of mature silique even after all the floral organs had abscised.

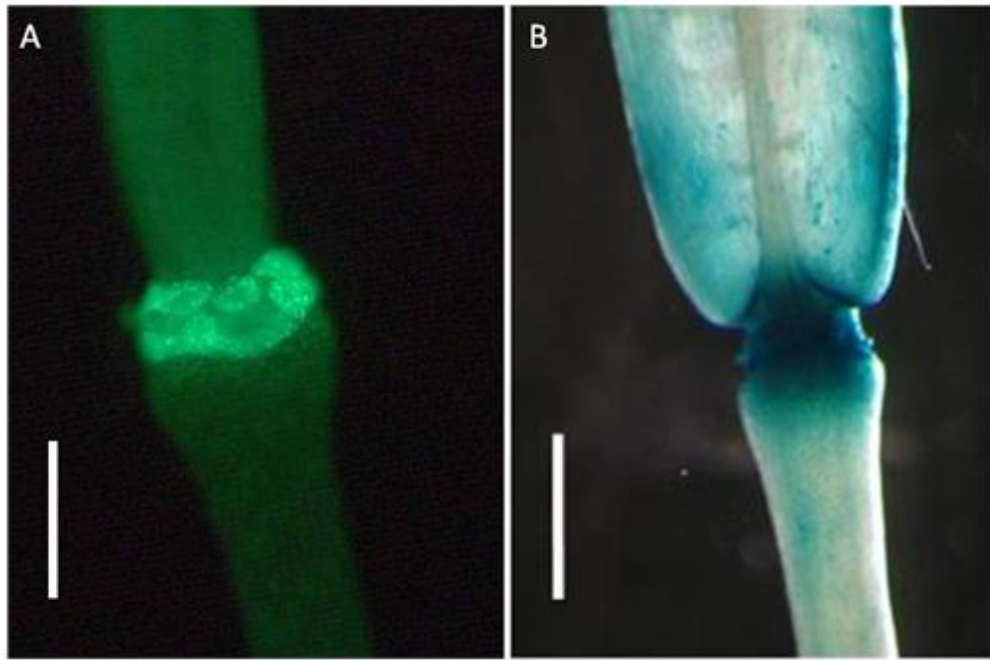


**Figure 3.4** *G2:GFP* and *G2:GUS* expression in the abscission zone of the flower at position 8 (A) and position 10 (B) of *Arabidopsis*. Scale bar: 1 mm. **(A)** *G2:GFP*; **(B)** *G2:GUS* (Shahid and González-Carranza, unpublished data).

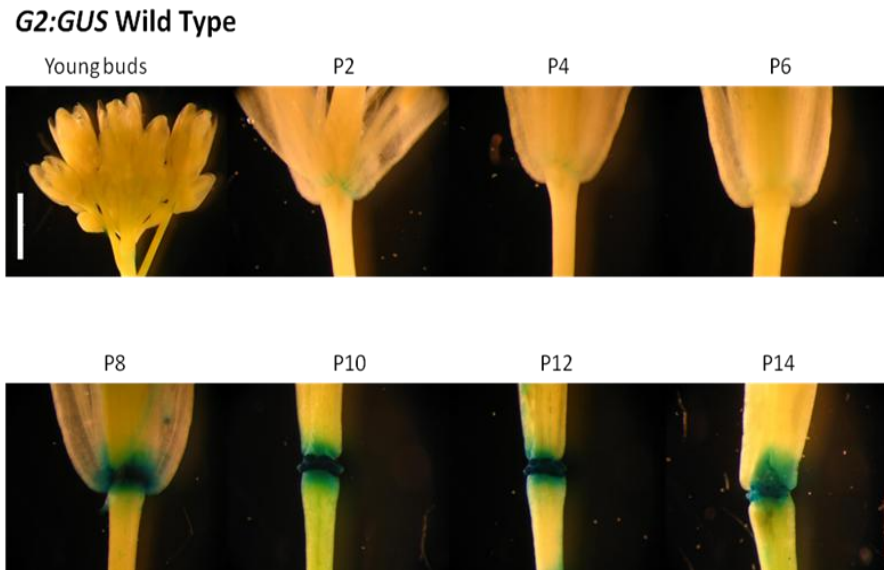


**Figure 3.5** Time course of *G2:GUS* expression. The expression commences in the AZ cells at position 2 (P2) and achieves strongest expression by position 8 (P8), which is also normally the position when wild-type *Arabidopsis* completes shedding of floral organs. The expression starts to decrease from position 14. Scale bar: 1 mm.

To determine which cells were expressing *G2* during abscission, *G2:GFP* floral organs from a *G2<sub>Prom</sub>::GFP* line were analyzed by a Confocal microscopy (Figure 3.6). Confocal microscopy was conducted using a Leica SP5 Confocal Laser Scanning Microscope (Leica Microsystems<sup>TM</sup>). Scanning settings were optimised and kept unchanged throughout the experiment. The green channel (GFP) was excited using the 488 nm line of an Argon laser and captured between 500 and 530 nm. The red channel (chlorophyll autofluorescence) was excited using the 488 nm line of the Argon laser and captured between

610 and 675 nm. Images were processed using Fiji (Fiji Is Just ImageJ 1.45r). *G2:GFP* signal commenced in the AZ cells at flower position 4 or 5. The strongest expression was observed at position 6 – 7 when the floral organs were shed (Figure 3.3a). *G2<sub>Prom</sub>::GFP* expression is highlighted in figure 3.6b, which shows that *G2* is expressed specifically in AZ cells. A 3D video showing specific *G2:GFP* expression in AZ is enclosed (supplemental CD).

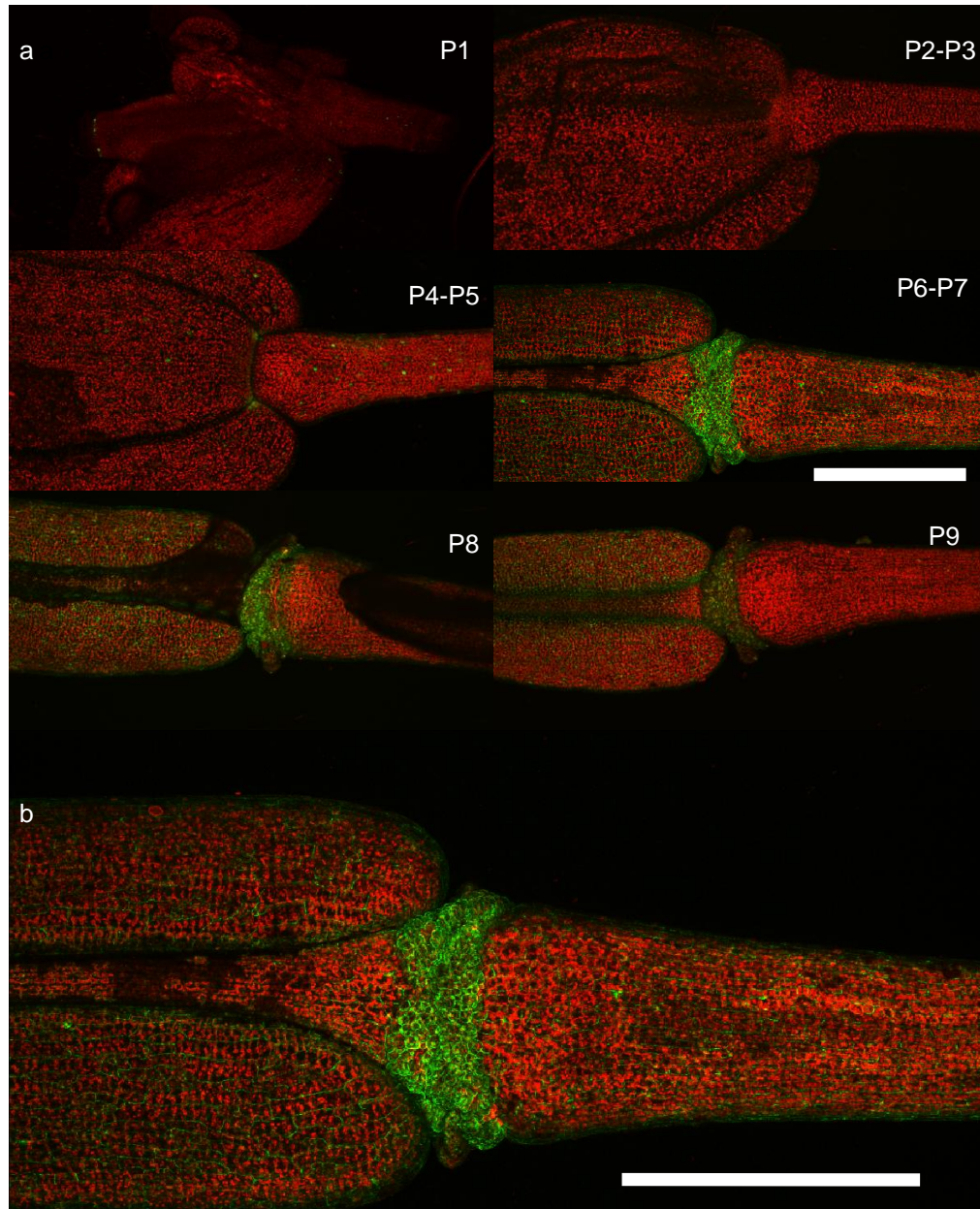


**Figure 3.6:** Confocal imaging of the time course of *G2<sub>Prom</sub>::GFP* expression (a) and a highlight of G2 expression at position 6 (P6) – P7 (b). (a) The expression commences in the AZ cells at P4 – P5 and achieves strongest expression by P6 –P7 when floral organs have been shed. (b) Increased magnification of G2 expression at position 6 (P6) – P7. Scale bar: 1 mm.

The *G2:GFP* signal was not only found in the floral organ AZ but also in the cortical cells that surrounded the site of emergence of the lateral roots (Figure 3.7). It has been shown that there is a cell separation events taking place in the cortex of the root during the process of lateral root emergence (Peretto *et al.*, 1992). *G2:GFP* was also detected in the root cap and lateral root cap, where cell separation takes place. The above evidence suggests that *G2* may play an important role in cell separation.



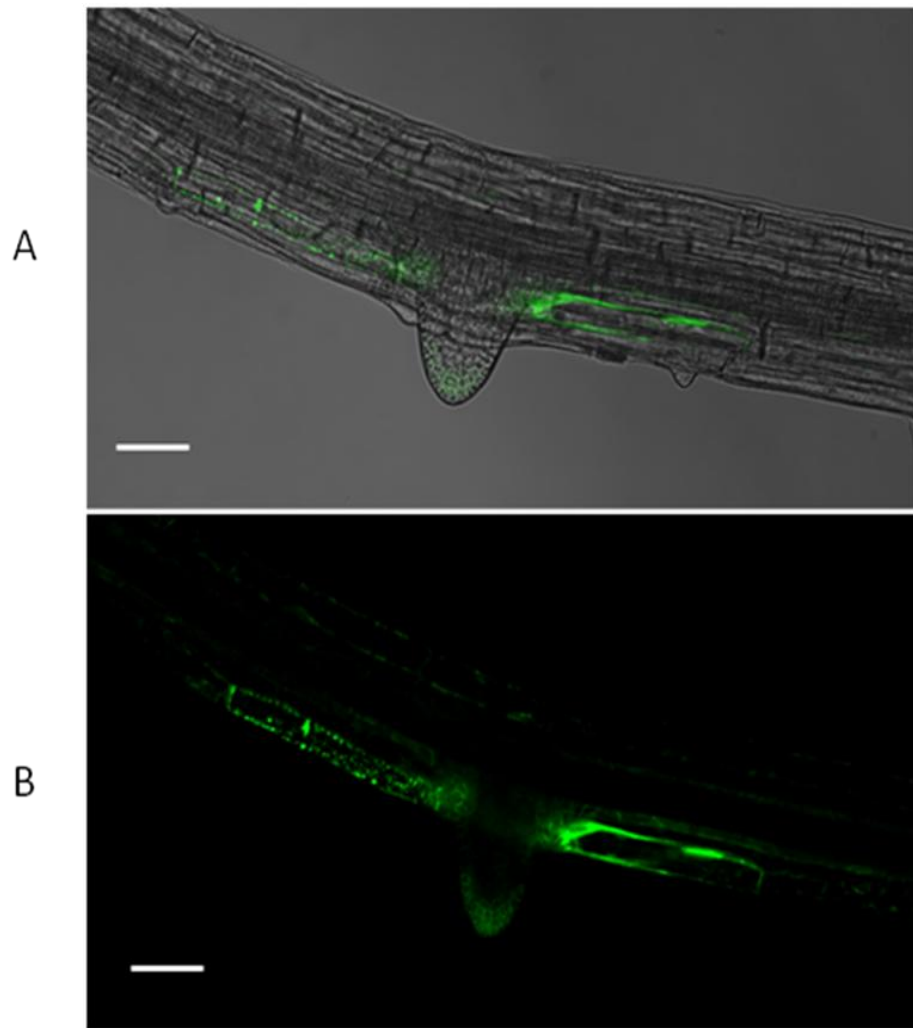


**Figure 3.7:** *G2:GFP* expression in root tissue. GFP expression in the lateral root cap and cortical cells that are surrounding the lateral roots emerging sites. **A** shows the *G2:GFP* signal with the root background and **B** shows the *G2:GFP* signal without background. Scale bar: 100 μm.

### **3.2.2 Spatial and temporal *G2:GUS* expression in three mutants in *Arabidopsis***

It has previously been shown that expression of *G2* is associated with the abscission of floral organs. To further investigate the correlation of expression pattern with abscission, the *G2:GUS* line was crossed into the mutants *ida*, 35S *IDA* and *bop1/bop2*. These genotypes show major differences in the timing of abscission.

Crossing was performed using a *G2:GUS* line as male and the three mutants lines as pollen recipients. The F3 plants were confirmed by PCR using *G2\_Pr\_forward* and *GUS\_sequence* primers (Table 1.1). The PCR positive plants with the mutant phenotypes were selected and analysed for spatial & temporal GUS expression (Figure 3.4).

#### **3.2.2.1 Crossing *G2:GUS* with *inflorescence deficient in abscission (ida)***

Flowers of the mutant *inflorescence deficient in abscission (ida)* remain attached to the plant body throughout pod development and seed shedding (Butenko *et al.*, 2003). The absence of IDA results in an incomplete dissolution of the middle lamella in AZ cells in plant (Butenko *et al.*, 2003).

The crossing was performed using *G2:GUS* homozygous line as the pollen donor. The F2 lines were screened by GUS expression and *ida* phenotypes - individuals having both genotypes were selected for the GUS analysis.

*G2:GUS* expression in a homozygous *ida* background could be detected at the base of floral organs from position 8 but the expression level is significant lower than which is at the position 8 in a wild type background. The *GUS* reached maximum at position 10, whereas in wild type it is position 8 (Figure 3.4). Expression was therefore delayed and did not reach the same intensity of expression as in wild type.

### **3.2.2.2 Crossing *G2:GUS* with *35S:IDA***

Overexpression of *IDA* leads to ectopic cell separation, an increasing number of AZ cells, and much earlier abscission from position 2 – 3 (Stenvik, *et al.*, 2006). In addition, cell separation was seen at the base of pedicels, branches and cauline leaves. It has been suggested that these might represent vestigial AZs. Secreted Arabinogalactan-Protein (AGP) was also detected covering the AZ (Stenvik *et al.*, 2006).

The crossing was performed using the homozygous *G2:GUS* as pollen donor. In F2 progenies, individuals with both GUS expression and *35S:IDA* phenotype were selected. The F3 lines with 100% individuals having both GUS expression and *35S:IDA* were studied in detail.

In the *35S:IDA* background, the *G2:GUS* expression occurs at position 4, which is much earlier than wild-type, in which *G2:GUS* expression occurs at position 8. In addition, the *G2:GUS* expression is much more extensive (Figure 3.4).

### **3.2.2.3 Crossing *G2:GUS* with *blade-on-petiole1* & *blade-on-petiole2* (*bop1/bop2*)**

The *BLADE-ON-PETIOLE1* & *BLADE-ON-PETIOLE2* (*BOP1* & *BOP2*) genes play a key role in AZ differentiation (Ha *et al.*, 2007; McKim *et al.*, 2008). Plants lacking *BOP1/BOP2* have been suggested to fail to differentiate an abscission zone (Hepworth *et al.*, 2005). In order to determine whether *G2* is expressed in plants that fail to abscise, *G2:GUS* was crossed into *bop1/bop2* double mutant material.

The crossing was performed using *G2:GUS* as pollen donor and *bop1/bop2* double mutant as the pollen recipient. The F2 progenies

were grown in a tray with 96 wells and individuals with both GUS expression and *bop1/bop2* phenotypes were selected for GUS expression analysis.

*G2:GUS* expression in *bop1/bop2*, although no abscission took place, could be detected from position 12 (Figure 3.8). The level of expression was much weaker than in wild type plants and was observed at a much later stage of floral development.

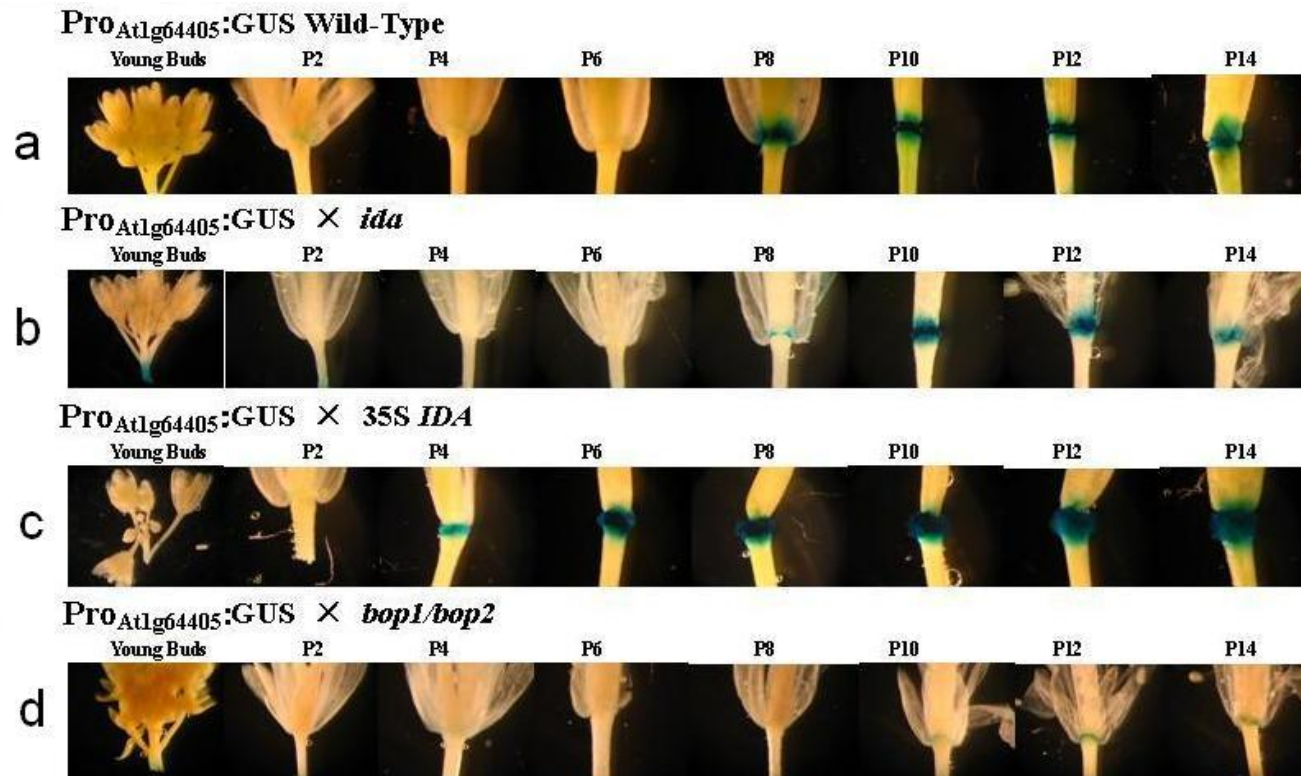


**Figure 3.8** Time course of G2 expression during flower development: (a): The *Pro<sub>Atlg64405</sub>:GUS* (*G2:GUS*) expression in wild-type background. The expression in the wild-type background initiated from position 2 (P2). (b): The *G2:GUS* expression in *ida* background started from position 8 (P8) and reached the highest expression at positions 10 to 12, which shows a delay. (c): The *G2:GUS* in the *35S:IDA* background showed both an earlier and a much more intense expression pattern compared to the wild-type. (d): In *bop1/bop2* plants, the expression was undetectable until position 8 and then slight expression commenced from position 10 (P10).

#### 3.2.2.4 Wounding-related expression of *G2:GUS*

*G2:GUS* expression is strongly up-regulated by wounding and is restricted to the wounded sites. Mature cauline leaves from wild type plants were wounded by needle and incubated at room temperature for 30 min before being assayed for GUS activity. Accumulation of GUS was detected at the site of wounding (Figure 3.9).

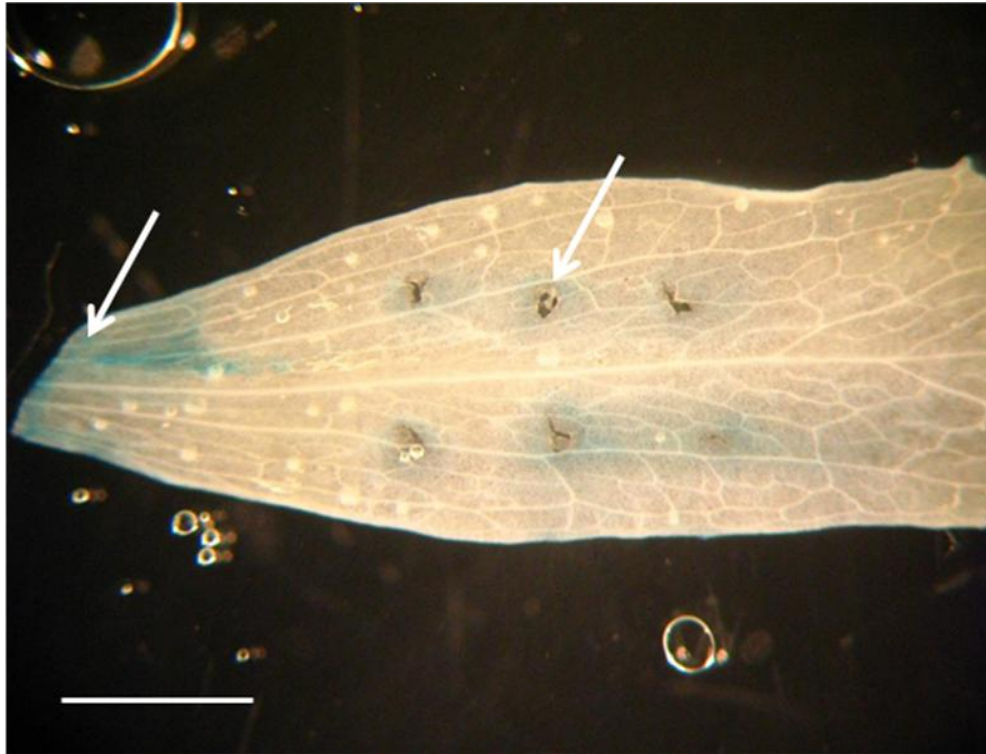


**Figure 3.9** Wound-induced expression of *G2:GUS* in a cauline leaf. Arrows show the wounded sites and sites of *G2:GUS* expression. Scale bar: 50 mm.

The wound induced expression of *G2:GUS* was studied in *ida* and *35S:IDA* backgrounds. Figure 3.10a shows the *G2:GUS* expression at the wounded site of the pedicel at different stages of flower development in wild type. In an *ida* background *G2:GUS* expression was more diffuse (Figure 3.10b). The wounding did not induce GUS expression at the base of the pedicel tissue in *35S:IDA* background (Figure 3.10c).

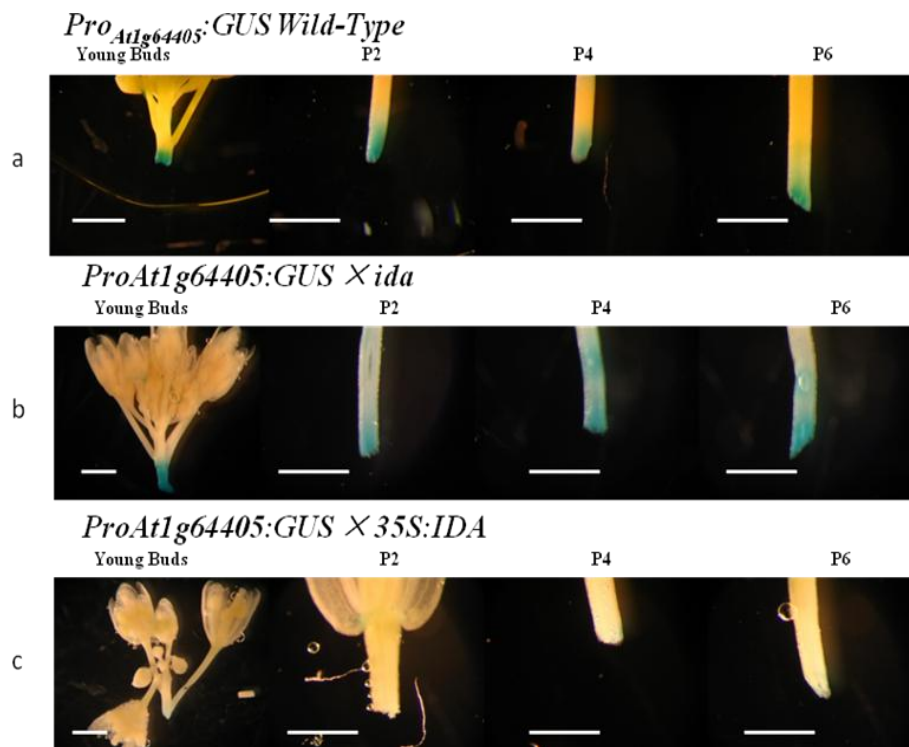


**Figure 3.10** Wound-induced expression of *G2:GUS* (*ProAt1g64405:GUS*) in different genetic backgrounds. (a) wild-type, (b) *ida*, (c) *35S IDA*. Scale bar: 1 mm.



Expression of *G2:GUS* can be seen in the cells at lateral root emerging sites and the *G2:GUS* signal can be observed to be diffused (Figure 3.11). In an *ida* background, *G2:GUS* gave a much stronger expression and covered more of the root compared to the wild type. In *35S:IDA* background, the GUS signal was absent.

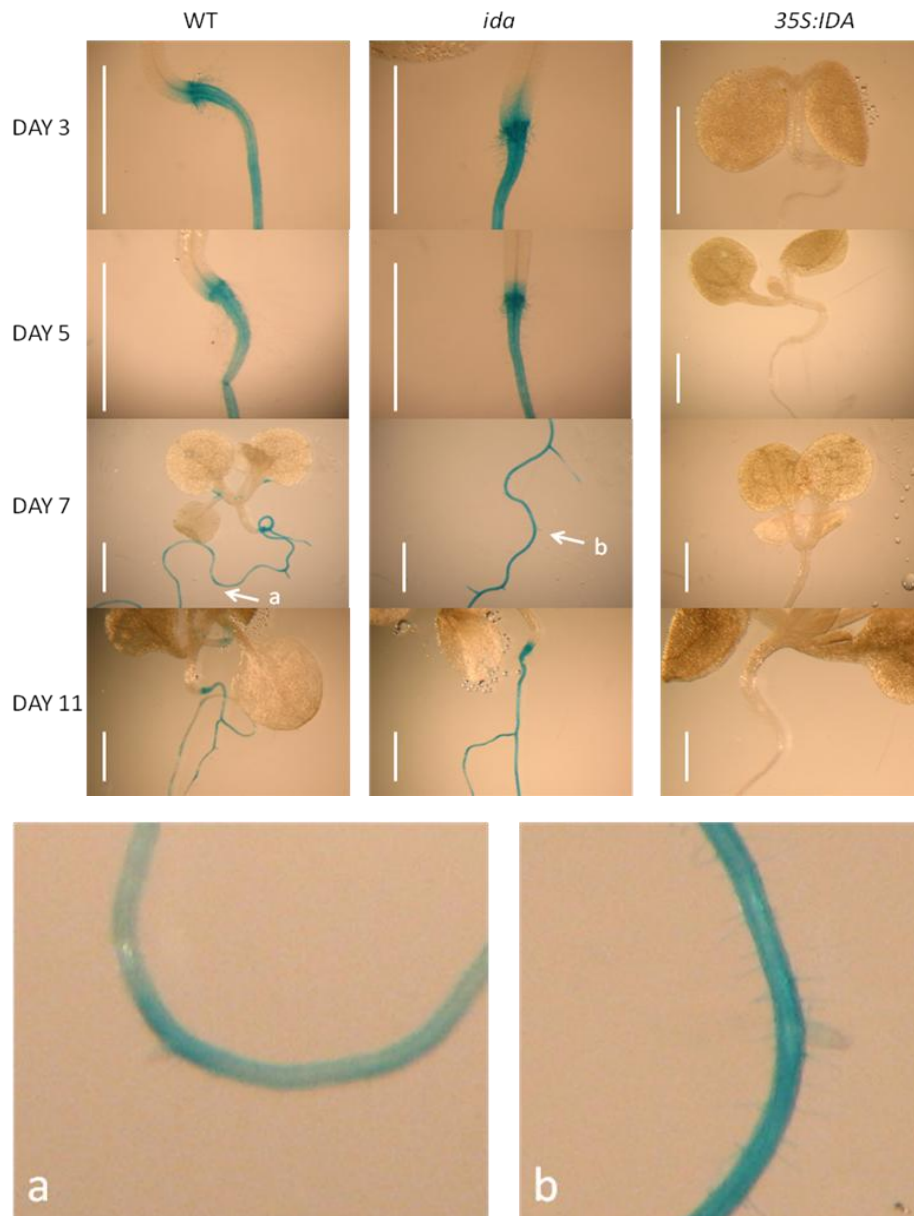


**Figure 3.11** *G2:GUS* expression in roots tissues in the wild type, *ida* and *35S:IDA* backgrounds. **WT**: wild type. **Day 3 – Day 11** indicate 3 day to 11 day old *Arabidopsis* seedlings. The area indicated by arrows **a** and **b** are the fourth lateral roots of wild type (**a**) and *ida* (**b**) plants, which are highlighted in Figure 3.7a and 3.7b. Scale bar: 1 mm.

This expression analysis indicates a negative correlation between *IDA* and *G2*. Up-regulation of *IDA* leads to a down-regulation of *G2*

expression in roots and associated with wounding in the base of pedicel.

A microarray analysis was undertaken to study the correlation between *IDA* and *G2* expression in other tissues using data from the Two Gene Scatter Plot of NASC array (<http://affymetrix.Arabidopsis.info/narrays/twogenescatter.pl>) and further evidence to support an inverse correlation can be seen (Figure 3.11). Each dot in figure 3.8 represents one micro array slide and the positions of the dots show the expression value of *G2* (*x*) and *IDA* (*y*).

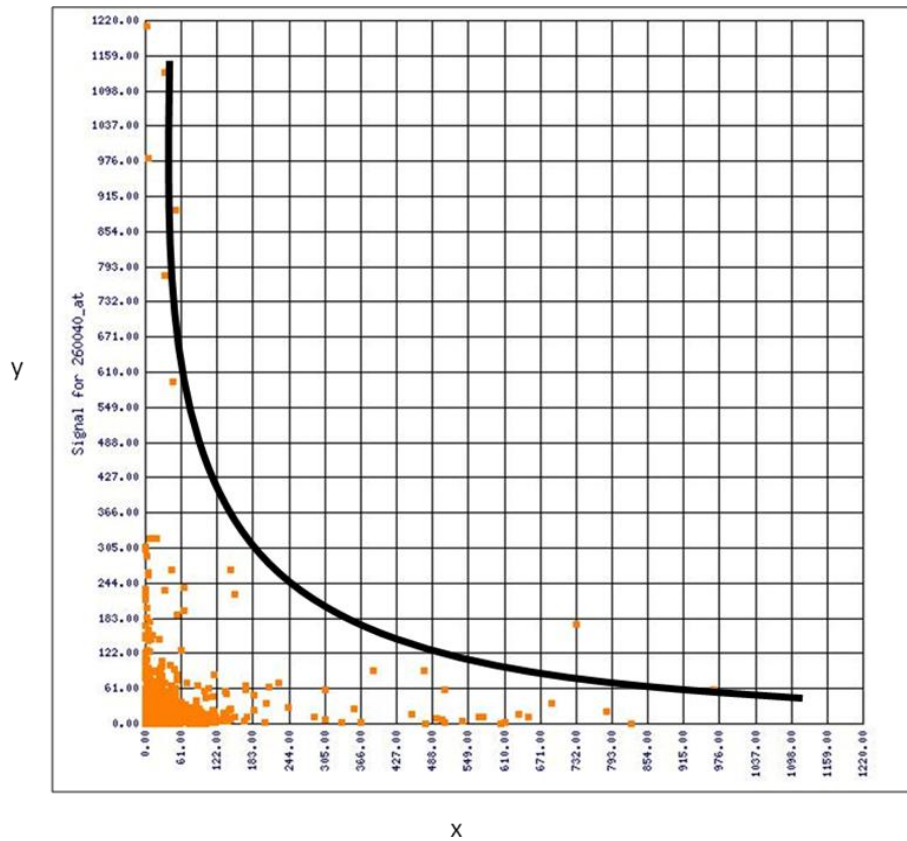


**Figure 3.12** NASC array Two Genes Scatter Plot of the correlation between *G2* and *IDA*. Each dot represents one micro array slide. (**x**) Expression value of *G2*. (**y**) Expression value of *IDA*.

*G2:GUS* expression was also studied in the root cap of plant materials. Interestingly, *G2:GUS* expression in root caps was not affected or even enhanced by overexpression of *IDA* (3.13).

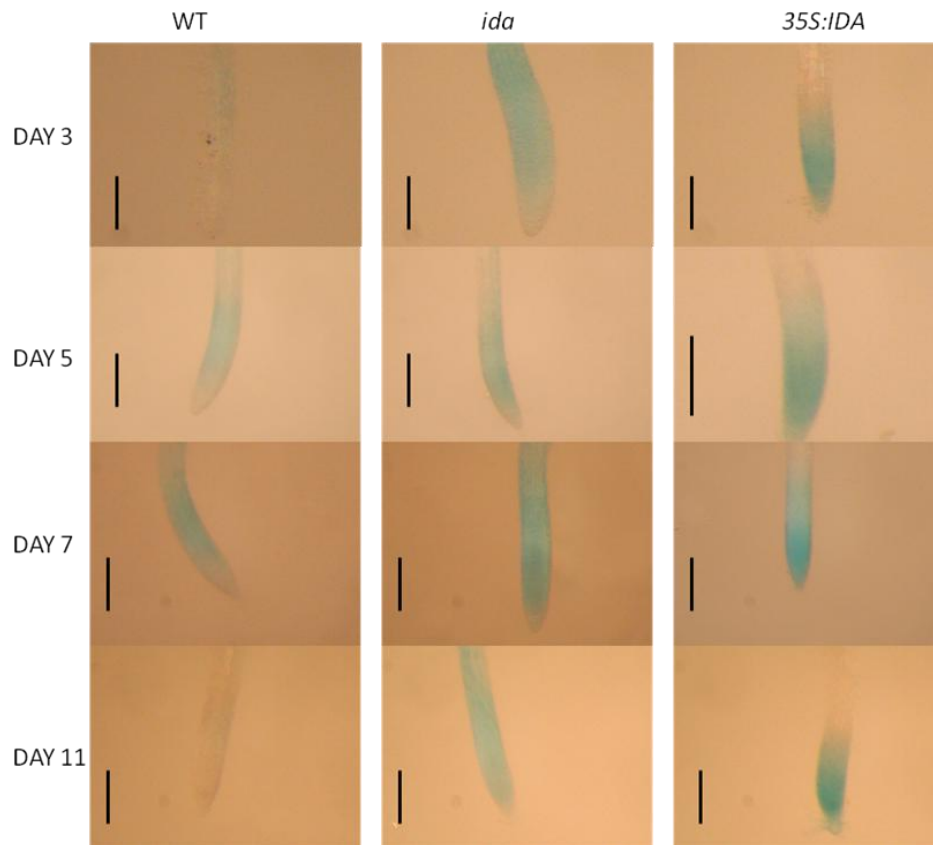


**Figure 3.13** *G2:GUS* expression in the root tips of wild type, *ida* and 35S:IDA backgrounds. **WT:** wild type. **Day 3 – Day 11** indicate 3 day to 11 day old *Arabidopsis* seedlings. Scale bar: 250  $\mu$ m.

### 3.3 Bioinformatic analysis of G2 gene and protein

The DNA/protein information of G2 is available in The *Arabidopsis* Information Resource (TAIR). A WU-BLAST analysis using G2 cDNA sequence as a probe showed that G2 is a unique gene in *Arabidopsis* with an unknown function. G2 was analyzed in an *in-silico* analysis tool Genevestigator\_V3 (<https://www.genevestigator.ethz.ch>) and the expression pattern predicted was correlated with our lab-based gene expression analysis. Protein database Simple Modular Architecture Research Tool (SMART) (Schultz *et al.*, 1998; Letunic *et al.*, 2008) was employed to study the G2 protein sequence but no predicted functional motif was found.

In order to understand more about G2, further bioinformatics analysis was carried out by using various online tools/databases. Genevestigator\_V3 database can provide gene expression patterns in different organs, growth stages and environmental conditions through Affymetrix GeneChip data (Zimmermann *et al.*, 2004). For the analysis in terms of protein structure, the online tool ExPASy (Expert Protein Analysis System) (<http://expasy.org/tools/>) (Gasteiger *et al.*, 2003) was employed. ExPASy is a proteomics server supplying various tools in analyzing protein sequences and structures, such as “Translate” for translating a nucleotide sequence to a protein sequence, “ProtScale” for hydrophobicity of amino acids and “Myristoylator” for prediction of N-terminal myristoylation by

neural network. Protein Homology/analogy Recognition Engine (PHYRE) is a good online server for prediction of secondary structure of a protein sequence (<http://www.sbg.bio.ic.ac.uk/~phyre/>) (Kelley and Sternberg, 2009), which is also employed in this study of G2 protein secondary structure.

### **3.3.1 G2 gene expression pattern predicted by Genevestigator\_V3**

The expression pattern of G2 in different tissues and different development stages was analyzed by using Genevestigator\_V3 (<https://www.genevestigator.ethz.ch>).

For G2 expression in different tissues, Gene Atlas Tool (Anatomy) from Genevestigator\_V3 was employed (Fig 3.13). ATH1:22K array from wild type *Arabidopsis* was selected as array type and the AGI code of G2 “At1g64405” was submitted as the gene of interest. The x axis showed the expression value and the y axis showed different tissues types. The data show that the G2 expression level was low in the majority of the tissues/organs but significantly higher in the AZ. An intermediate level of expression was observed in hypocotyl, radicle, carpel, stamen, lateral root, root tip and root hair zone.

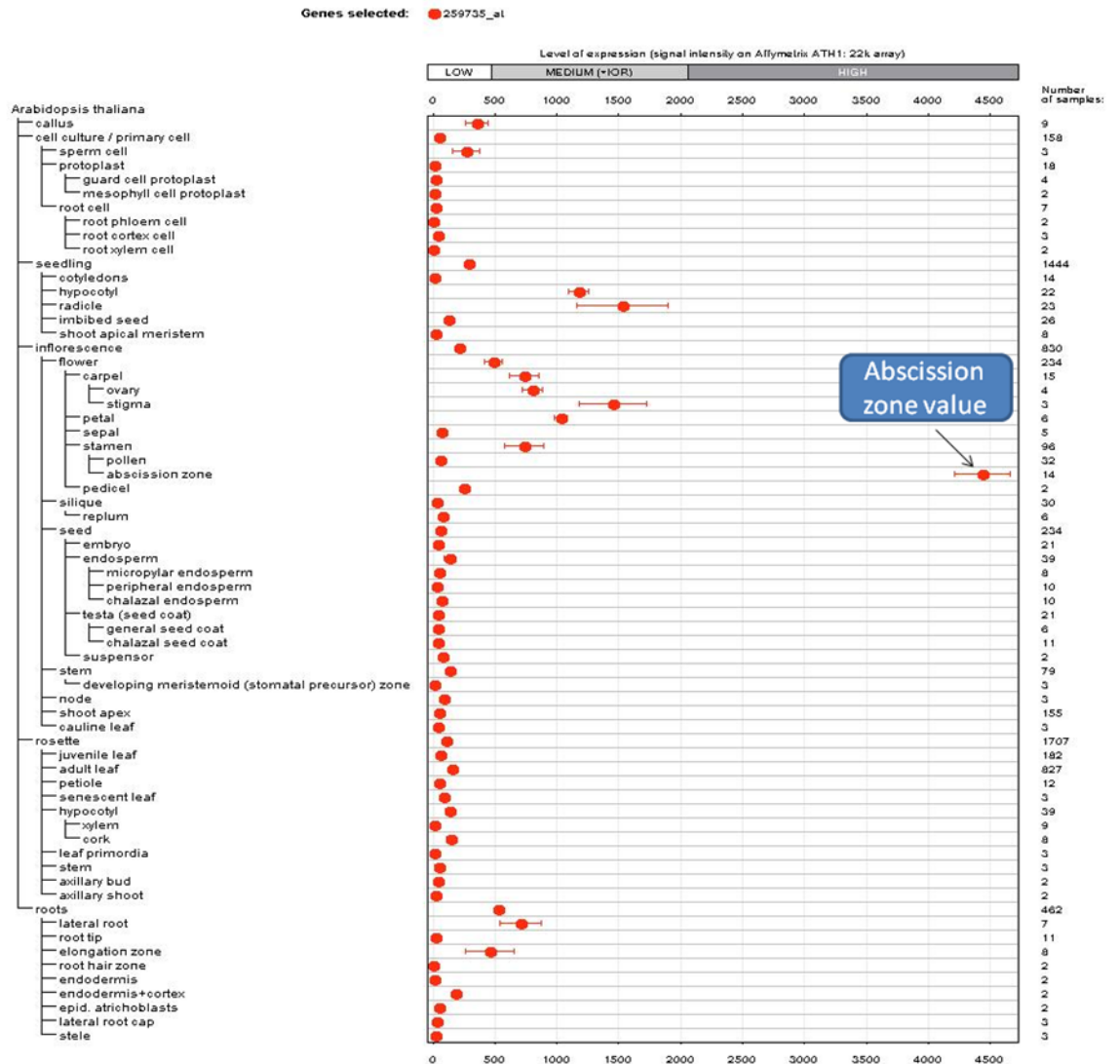


**Figure 3.14** G2 expression value in different tissues in *Arabidopsis* from Genevestigator V3 (Anatomy). G2 shows a significant high level of expression in AZ, medium level of expression in hypocotyl, radicle, carpel, pollen, lateral root, root tip and root hair zone.

To analyze G2 expression profile in various development stages, another tool, Gene Chronology from Genevestigator\_V3 was employed. The data show that G2 is expressed at a low level in all development stages and expressed in germinating seedling, seedling and flower & siliqua (Figure 3.15).



Genes selected: ● 259735\_at

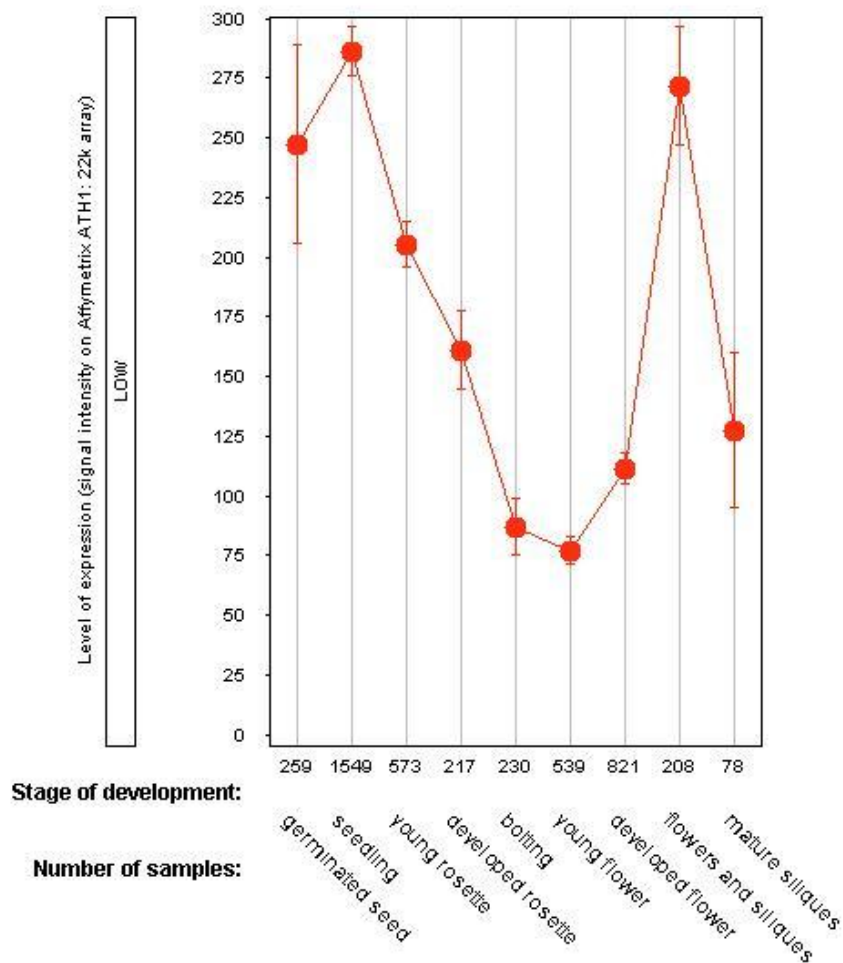


**Figure 3.15** G2 expression pattern at different developmental stages shown by Gene Chronology tool from Genevestigator\_V3. ATH1:22K array from wild type *Arabidopsis* was selected as array type and the AGI code of G2 “At1g64405” was submitted as the gene of interest. The value in the x axis indicates the number of array experiments. The average expression level of G2 is shown as “low”.

### 3.3.2 Identification of putative orthologues of G2

In order to search for potential orthologues of G2, a WU-BLAST (<http://www.Arabidopsis.org/wublast/index2.jsp>) search using G2 genomic DNA provided by TAIR was carried out. The WU-BLAST search in *Arabidopsis* showed that the best match gene, *At5g37430*, shared 60%

similarity with the score 218 and P value 0.00044, and both of the values were relatively low. The WU-BLAST results indicated that G2 is a unique gene in *Arabidopsis*. The G2 nucleotide sequence was then sent to TBLASTX in NCBI (<http://blast.ncbi.nlm.nih.gov/Blast.cgi>). TBLASTX search is another program in BLAST family and it translates the query nucleotide sequence in all six possible frames and compares it against the six-frame translations of a nucleotide sequence database. The result showed that a gene in *Arabidopsis lyrata*, was identified as putative G2 orthologue (Table 3.1).

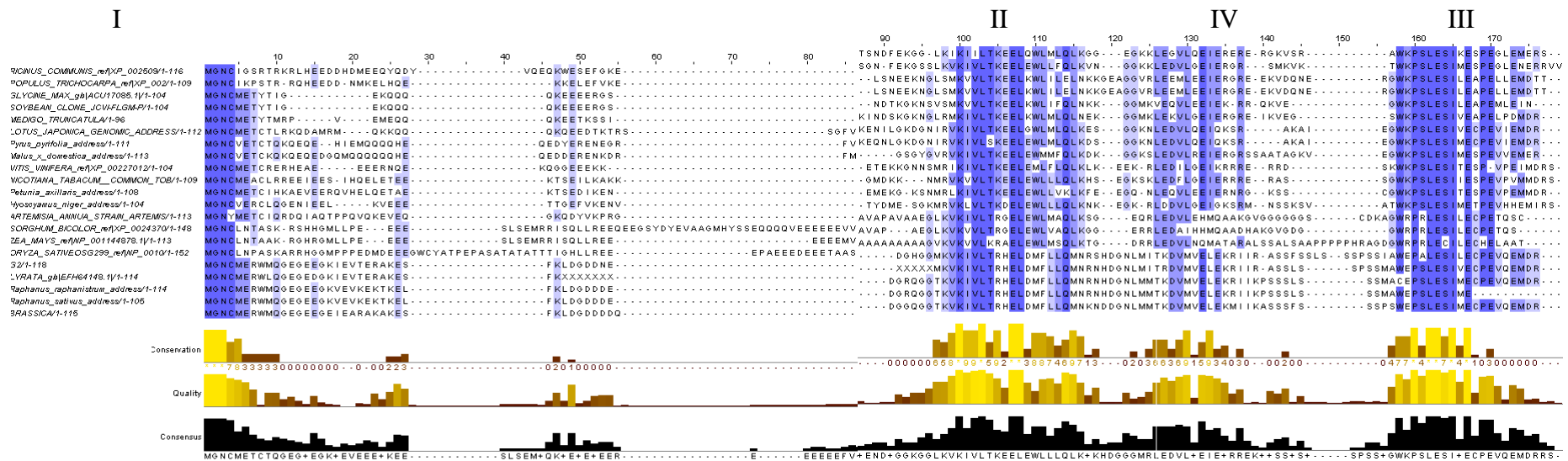
Gene ID	Description	Score	E-Value
<i>At1g64405</i> (G2)	<i>Arabidopsis thaliana</i> unknown protein (AT1G64405) mRNA	1284	$7e^{-74}$
9323952	<i>Arabidopsis lyrata</i> subsp. <i>lyrata</i> hypothetical protein	1087	$1e^{-57}$

**Table 3.1** TBLASTX analysis result using G2 nucleotide sequence as a probe. The data showed a gene from *Arabidopsis lyrata* has the most similarity to G2.

Another three genes from *Brassica*, *Raphanus raphanistrum*, and *Raphanus sativus* respectively were then selected as potential orthologues of G2 by using BLAST from respective databases. An alignment analysis was then carried out among the five protein sequences by using ClustalW 2.1 online tool (<http://www.ebi.ac.uk/Tools/msa/clustalw2/>) (Chenna *et al.*, 2003; Larkin *et*

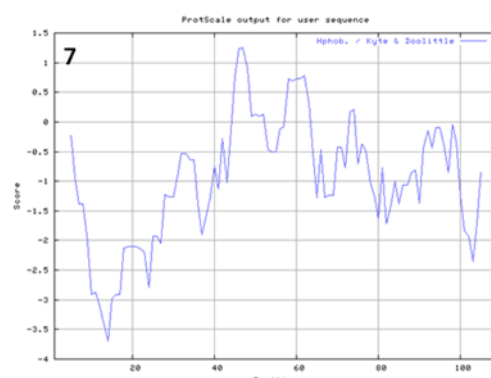
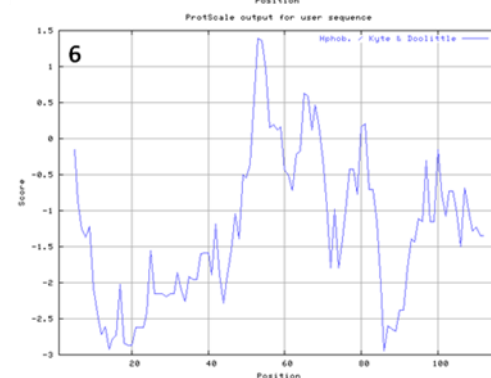
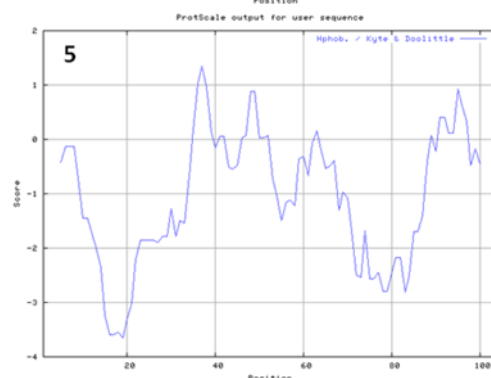
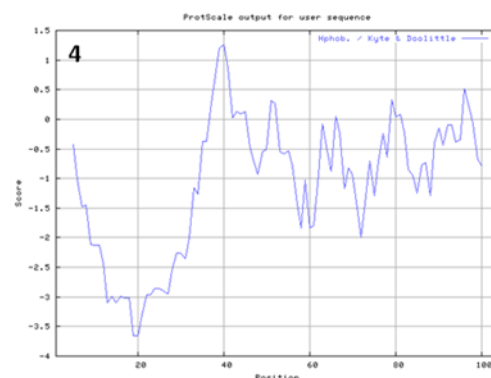
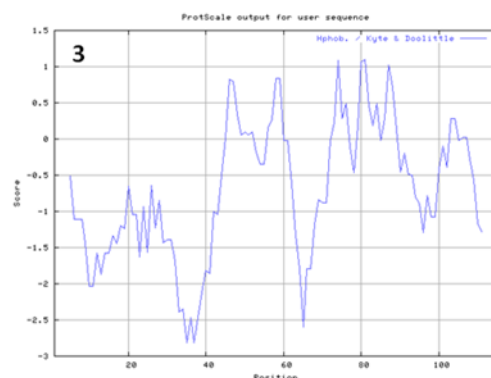
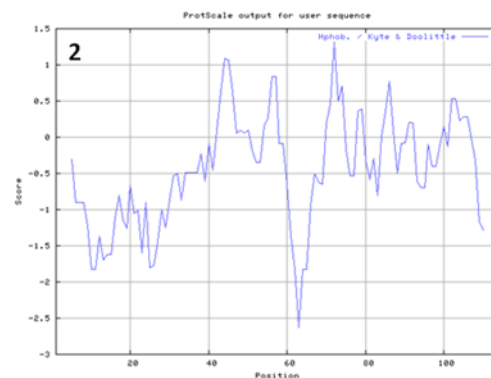
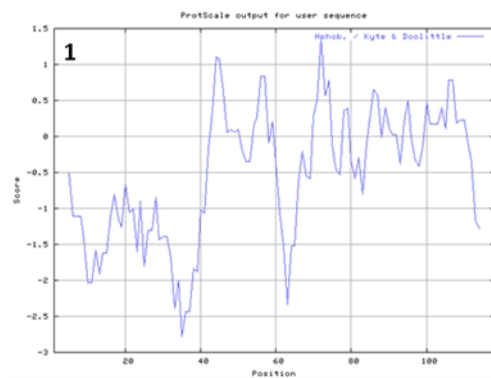


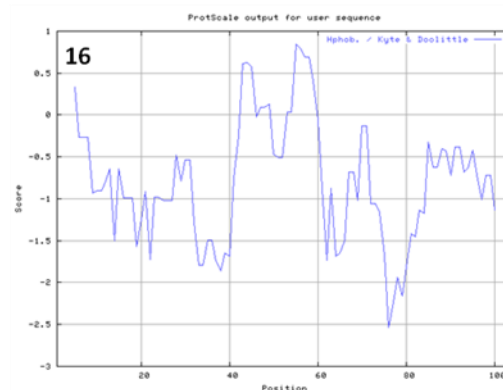
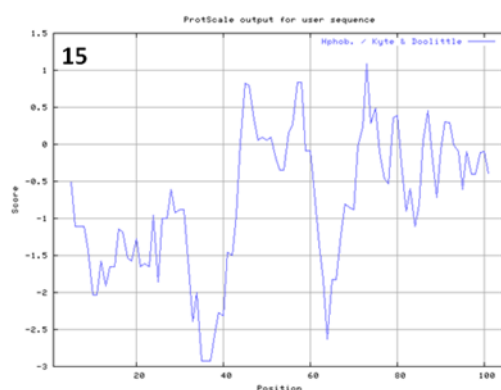
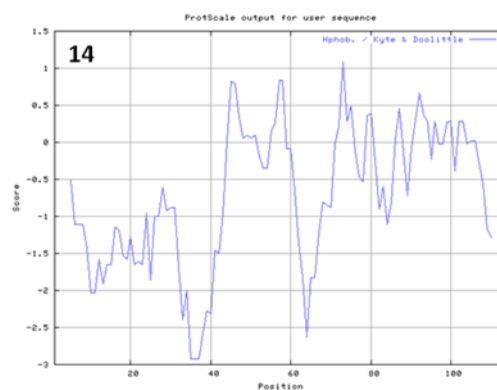
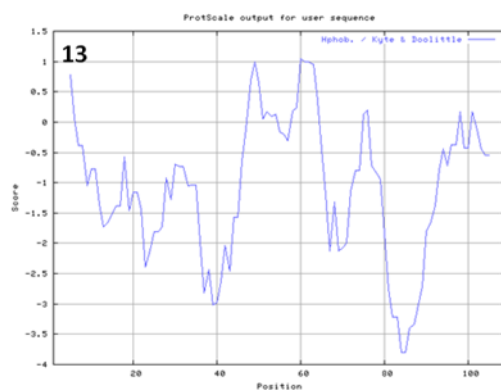
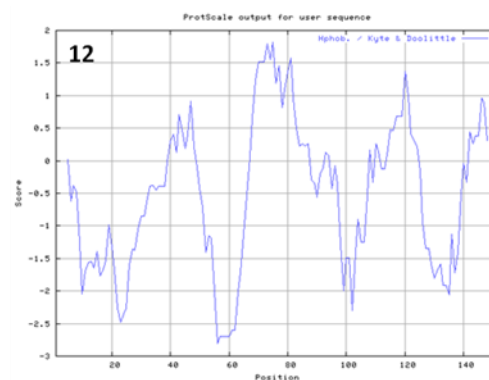
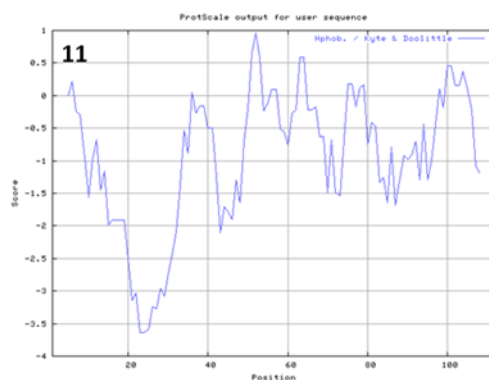
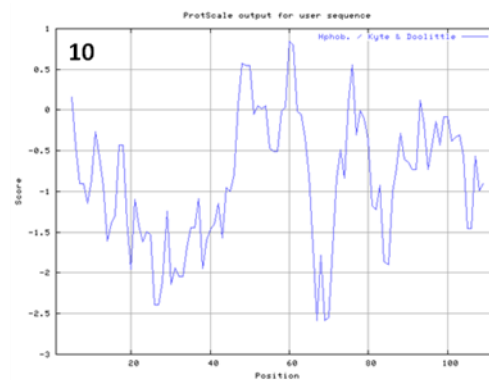
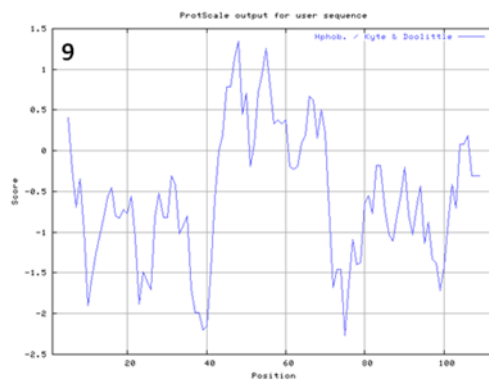
presented in figure 3.17. Interestingly, although TBLASTX hit scores for the majority of the nineteen proteins were significantly low, the nineteen proteins shared similar features with G2. The nineteen proteins are all functionally unknown and figure 3.13 shows that they not only have a similar length of about 100 amino acids but also share four conserved motifs with G2. The four motifs are located in the N terminal, the middle part of the sequence, and the C terminal. Three of the four motifs are significantly conserved: “MGNC”, “XKVKIVLXRXEL” and “WXPXLESIXE” marked as motif I, II and III, and the other motif is relatively conserved and marked as Motif IV (Figure 3.17).



**Figure 3.17** ClustalW alignment of the deduced amino acid from the translation start sites of ORF among G2 and nineteen genes from different species. Conserved regions are marked in blue colour. I – IV represent the 4 conserved motifs.

The sequences of the twenty genes were then analyzed for hydrophobicity by ProtScale in ExPASy (<http://expasy.org/tools/protscale.html>) using Hphob. / Kyte & Doolittle scale for measuring amino acid hydrophobicity (Kyte and Doolittle, 1982). Interestingly, the 20 protein sequences showed a similar trend in hydrophobicity (Figure 3.18).







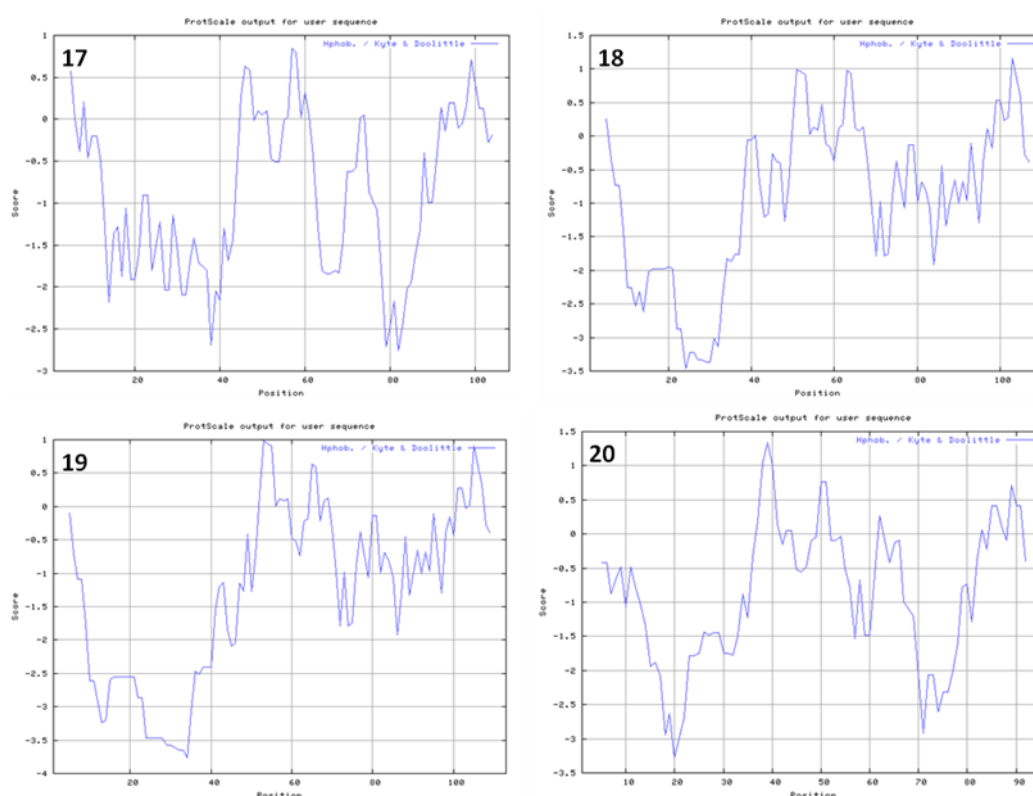


**Figure 3.18** Amino acids scales of hydrophobicity of the twenty deduced proteins sequences from Prot Scale tools of ExPASy. (x) axis represents the position of the amino acid in the protein sequence; (y) axis gives a represent of hydrophobicity value. (1) *G2*, (2) *Arabidopsis lyrata*, (3) *Brassica*, (4) *Vitis vinifera*, (5) *Glycine max*, (6) *Ricinus communis*, (7) *Populus Trichocarpa*, (8) *Sorghum bicolour*, (9) *Zea mays*, (10) *Artemisia annua strain artemis*, (11) *Lotus japonica*, (12) *Oryza sativa*, (13) *Nicotiana tabacum*, (14) *Raphanus raphanistrum*, (15) *Raphanus sativus*, (16) *Hyoscyamus niger*, (17) *Petunia axillaris*, (18) *Pyrus pyrifolia*, (19) *Malus domestica*, (20) *Medicago truncatula*.

In general, the 20 deduced proteins sequences showed similar features in terms of hydrophobicity. Firstly, all of the twenty proteins sequences showed a hydrophilic peak between amino acid position 10 – 40, despite this common feature that the amino acids in this part of the sequence varied. Secondly, all of the twenty proteins sequences showed a hydrophobic peak between amino acid position 40 – 60 (in *Sorghum*

*bicolour* 60 - 80), which is the location of motif II. Thirdly, after motif II there is a hydrophilic peak between amino acid 60 - 100 (in *Sorghum bicolour* 80 – 120). Finally, in the area of motif III, 13 of the 20 proteins sequences showed a low hydrophobic peak.

### **3.3.4 Protein secondary structure analysis**

The amino acids sequences of the twenty proteins were then sent to PHYRE (<http://www.sbg.bio.ic.ac.uk/~phyre/>) server in order to predict their secondary structure. The results showed that the major part of all the twenty proteins were alpha helixes with the first helix motif near the N' terminus, the second in motif II and the third in motif IV (Figure 3.19). All the proteins showed a conserved domain in motif II as a beta strand. 11 out of the 20 proteins showed predicted alpha helixes in motif III.

PHYRE server also provides a predictive model of the 3D structure of a protein. However with most of the twenty proteins (18 out of 20) the estimated precision score was low (less than 10%). The highest precision score is in *Zea mays* (35%) and *Sorghum bicolour* (30%), which are predicted to contain a spectrin repeats motif (Figure 3.20). Spectrin repeats are three-helix bundle structures contained in many proteins and it has been reported that they play an important role in coordination of cytoskeletal interactions with high spatial precision and serve as binding/interaction sites for many structural and signalling proteins (Djinovic-Carugo *et al.*, 2002). By using the online tool Myristoylator from ExPASy (<http://expasy.org/tools/myristoylator/>), G2 protein was predicted

to be involved in N-terminal myristoylation, which is an irreversible, co-translational protein modification. Except *Glycine max* and *Lotus japonica*, the rest of the nineteen protein were submitted to the online tool Myristoylator from ExPASy and they were also predicted as N-terminal myristoylated.

```

RICINUS_COMMUNIS_ref|XP_002509
POPULUS_TRICHOCARPA_ref|XP_002
GLYCINE_MAX_gb|ACU17085.1|
MEDIGO_TRUNCATULA
LOTUS_JAPONICA_GENOMIC_ADDRESS
Pyrus_pyrifolia_address
Malus_x_domestica_address
VITIS_VINIFERA_ref|XP_00227012
NICOTIANA_TABACUM_COMMON_TOBA
Petunia_axillaris_address
Hyoscyamus_niger_address
ARTEMISIA_ANNUA_STRAIN_ARTEMIS
SORGHUM_BICOLOR_ref|XP_0024370
ZEA_MAYS_ref|NP_001144878.1|
ORYZA_SATIVEOSG299_ref|NP_0010
G2
LYRATA_gb|EFH64148.1|
Raphanus_raphanistrum_address
Raphanus_sativus_address
BRASSICA

I
MGNCIGSRTRKRLHEEDDHDMEECYQDY----- 28
MGNCIKPSTK-RQHEEDD-NMKELHQE----- 25
MGNCMETYTI-----EKQOOQKEE----- 20
MGNCMETYTMRP-----VEMEQQQKEE----- 22
MGNCMETCTLRKQDAMRMQKKQQQKQE----- 27
MGNCVETCTCKQEQE--HIEMQQQOHE----- 25
MGNCVETCKQKQEQEDGQMQQQQQOHE----- 27
MGNCMETCRERHEA-----EEERNQE----- 22
MGNCMEACLRRREEEES-THQELETEEK----- 27
MGNCMETCIHKAEVEERQVHELOETAEK----- 28
MGNCMVERCLOGENIEEL-----KVEEET----- 23
MGNYMETCIQRDQIAQTPTQVQKEVEQG----- 28
MGNCCLNTASK-RSHHGMLLPE---EEE-----SLSEMRRISQL 34
MGNCCLNTAAK-RGHRGMLLPE---EEE-----SLSEMRRISQL 34
MGNCCLNPAKARHGGMPPEPDMDDEEGWCYATPEPASAATATTITIGHI 50
MGNCMERWMQGEEGEKIEVTERAKESF----- 28
MGNCMERWLQGEEDGKIEVTERAKESF----- 28
MGNCMERWMQGEEGEKVEVKETKELF----- 28
MGNCMERWMQGEEGEKVEVKETKELF----- 28
MGNCMERWMQGEEGEIEARAKAKESF----- 28
*** :

RICINUS_COMMUNIS_ref|XP_002509
POPULUS_TRICHOCARPA_ref|XP_002
GLYCINE_MAX_gb|ACU17085.1|
MEDIGO_TRUNCATULA
LOTUS_JAPONICA_GENOMIC_ADDRESS
Pyrus_pyrifolia_address
Malus_x_domestica_address
VITIS_VINIFERA_ref|XP_00227012
NICOTIANA_TABACUM_COMMON_TOBA
Petunia_axillaris_address
Hyoscyamus_niger_address
ARTEMISIA_ANNUA_STRAIN_ARTEMIS
SORGHUM_BICOLOR_ref|XP_0024370
ZEA_MAYS_ref|NP_001144878.1|
ORYZA_SATIVEOSG299_ref|NP_0010
G2
LYRATA_gb|EFH64148.1|
Raphanus_raphanistrum_address
Raphanus_sativus_address
BRASSICA

-----VQEQKWESEFGKETSNDFEKGG-LKIK 54
-----KKELEFVKESGN-FEKGSSLKVK 47
-----EERGS-----LSNEEKNGLSMK 37
-----TKSSI-----NDTKGKNVSMK 39
-----EDTKTRSSGFVKINDSKGKNGLRMK 52
-----QEDYERENEGRFVKENILGKDGNLRVK 52
-----QEDDERENKDRFMKEQNLGKDGNLRVK 54
-----KQGGEEEEK-----GSGYEVRYK 40
-----TSEILAKK-----ETEKKGNNSMRK 49
-----TSEDIKEN-----GMDKK---NMRVK 46
-----TGKLYENV-----EMEKG-KSNMRLK 44
-----KQDYVKPRG-----TYDME-SGKLRVK 49
LREEEQEEGSYDYEVAAAGMHYSSEQQQVEEEEVVAVAPAVAAHGLKVK 84
LREE-----EEEEMVAVAP---AEGLKVK 55
LREE-----EPAEEEEETAASAAAAAAAGVVK 82
-----KLDGDDNE-----DGHGGMKVK 45
-----LDGDDNG-----DGHGGMKVK 45
-----KLDGDDDE-----DGRQGGKVK 46
-----KLDGDDDE-----DGRQGGTGVK 46
-----KLDGDDDDQ-----DGGQGGTKVK 47
::*

II IV
ILTKKEELQWLMQLKGG---EGKKLEGLVQEIERERE-RGKVSR----- 95
IVLTKEELEWLLFQLKVN---GGKKLEDVLGEIERGR---SMKVK----- 86
VVLTKKEELKWLLILELNKGEAGGVRLMELEIERGRE-EKVDQNE----- 82
VVLTKKEELKWLLIFQLNRK---GGMKVEQVLEEIEK-RR-QKVE----- 77
IVLTKEELKWLMQLNLR---GGMKLEKVLGEIERGRE-IKVEG----- 92
IVLTKEELGWLMQLKES---GGKNLEDVLQEIQNSR-----AKAI----- 90
IVLSKEELEWLMQLKDS---GGKNLEDVLQEIQKSR-----AKAI----- 92
IVLTKEELEWMMFQLKDK---GGKSLVDVLEIERGRSSAATAGKV----- 83
IVLTKEELEWMLFLQLK---EEK-RLEDILGEIKRR---ERRD----- 87
VVLTKKEELEWLLQLKHS---EGKSKLEDVLEIERRR---ERRS----- 85
IVLTKEELEWLLVKLKF---EGQ-NLEQVLEEIERNR---GKSS----- 82
IVLTKEELEWLLQLKKN---EGK-RLEDVLGEIKSR---MNSKSKV----- 90
IVLTRGELEWLMQALKSG---EQRLDVDLEHMQAAAGVGGGGGGS----- 126
VVLTRGELEWLVQALKGG---ERRLEDVLEHMQAADHAKGVGDG----- 96
VVLKRAELEWLMSQLKTG---DRRLDVDLNMATARALSSAISAAPPPP 128
IVLTRHELDMLLQMNRRSHDGNLMTKDVMMVELEKRIIR-ASSFSLS-- 92
IVLTRHELDMLLQMNRRNHDGNLMTKDVMMVELEKRIIR-ASSLS----- 89
IVLTRHELDMLLQMNRRNHDGNLMTKDVMMVELEKRIIRIKPSSLS----- 91
IVLTRHELDMLLQMNRRNHDGNLMTKDVMMVELEKRIIRIKPSSLS----- 91
IVLTRHELDMLLQMNRRNHDGNLMTKDVMMVELEKRIIRIKPSSLS----- 92
::*: ** :. :: :.

```

```

                                III
RICINUS_COMMUNIS_ref|XP_002509      -----AWKPSLESIKESPEGLEMERS-- 116
POPULUS_TRICHOCARPA_ref|XP_002      -----TWKPSLESIMESPEGLENNERRVV 109
GLYCINE_MAX_gb|ACU17085.1|          -----RGWKPSLESILEAPELEMDTT-- 104
MEDIGO_TRUNCATULA                    -----GWKPSLESILEAPEMLEIN---- 96
LOTUS_JAPONICA_GENOMIC_ADDRESS      -----SWKPSLESIVEAPELPMDR--- 112
Pyrus_pyrifolia_address              -----EGWKPSLESIVECFEVIEMDR--- 111
Malus_x_domestica_address            -----EGWKPSLESIMECEPEVIEMDR--- 113
VITIS_VINIFERA_ref|XP_00227012      -----EGWKPSLESIMESPEVVEMER--- 104
NICOTIANA_TABACUM_COMMON_TOBA       -----SKWKPSLESITESP-VPEIMDRS- 109
Petunia_axillaris_address            -----SGWKPSLESITESPEVPVMDRS- 108
Hyoscyamus_niger_address             -----CGWKPSLESITESPEVPVMDR-- 104
ARTEMISIA_ANNUA_STRAIN_ARTEMIS      -----ATWKPSLESIMETPEVHEMIRS- 113
SORGHUM_BICOLOR_ref|XP_0024370      --CDKAGWRPRLESILECPETQSC----- 148
ZEA_MAYS_ref|NP_001144878.1|         -----GWRPRLESILECPETQS----- 113
ORYZA_SATIVEOSG299_ref|NP_0010     PHRAGDGWRPRLESILECHELAAT----- 152
G2                                   SSPSSIAWEPALESILECEPEVQEMDR--- 118
LYRATA_gb|EFH64148.1|               -SPSSMAWEPSLESIVECEPEVQEMDR--- 114
Raphanus_raphanistrum_address        ---SSMACEPSLESIMECEPEVQEMDR--- 114
Raphanus_sativus_address             ---SSMAWEPSLESIME----- 105
BRASSICA                             ---SSPSWEPSLESIMECEPEVQEMDR--- 115
                                . * * * . * *

```

**Figure 3.19** Predicted secondary structure of the twenty proteins with the background of ClustalW alignments. **Alpha helixes** are presented in red. **Beta strands** are presented in blue. Amino acids without background colour are predicted as **coils**. Each amino acid has a predicted score from 1 - 10 for the probability of the confidence (Data not shown). “\*” indicates that the residues in that column are identical in all sequences in the alignment. “:” indicates that a conserved substitution has been observed. “.” indicates that semi-conservative substitutions have been observed. Score of probability which are greater than 5 were selected. I – IV represent the 4 conserved motifs.



**Figure 3.20** A cartoon picture of the 3D structure of the deduced protein of *Zea mays* predicted by PHYRE server. **Alpha helixes** are shown in red. **Beta strands** are shown in blue. **Coils** are shown in white.

The twenty protein sequences including G2 were also sent to online tools such as ExPASy and SMART in order to search for putative functional domains. The result suggested that no putative functional domain was found. The TMHMM Server 2.0 was used in prediction of transmembrane helices in the twenty proteins and the predicted location of the intervening loop regions (<http://www.cbs.dtu.dk/services/TMHMM>) (Krogh *et al.*, 2001). The result showed that the twenty proteins appeared to have no transmembrane helix.

### 3.3.5 G2 protein sequence has 2 motifs in N' and C' terminal that are conserved with 9 *Arabidopsis thaliana* proteins.

The four putative motifs were then sent as probes to online tool Patmatch in TAIR (<http://www.Arabidopsis.org/cgi-bin/patmatch/nph-patmatch.pl>) in order to search *Arabidopsis* genes that may share these motifs with G2. The result showed that 9 genes have motif I and III conserved with G2 (Figure 3.21).

	I	
at1g10530	MGNCQAVNAAVLVLPQHPGG-IIDRYYSVSVTEVMAMYPGHY--VSLIIPLSEEEKNIP	57
at1g60010	MGNCQAVDAAALVLQHPDG-KIDRYYGPSVSEIMRMPGHY--VSLIIPLP---EKNIP	54
at5g50090	MGNCQAVDTARVVIQHPNG-KEEKLSCPVSASYVMKMNPGHC--VSL-----IS	47
at5g62900	MGNCQAAEAATTVIQQPDG-KSVRFYCTVNASEVIKSHPGHH--VALL-----LS	47
at5g67620	MGNCQAAEAATVLIHHPAENKVERIYWSVTASDIMKSNPGHY--VAVV-----VT	48
at5g03890	MGNCLVMEKKVIKIVRDDG-KVLEYREPISVHHILTQFSGHS--ISHN-----N	46
at3G21680	MGNCLRHDNGVARKEKDDLDPEPLVKLLEEGKTSFRGEESE--RSTE-----	46
at3G20340	MGNCLRHESEMHWAGEDWDEFITEDEEDHHYSSKTRDGKPV--IVTR-----	46
at4G21920	MGNCICVTEKTTTSWGGDDNGSYNRRRRRSTVVHDDNDG--EKLIG-----E	48
G2	MGNCMER----WMQGEEGEGKIEVTERAKESFKLDGDDNEDGHGG-----	41
	****	
at1g10530	ATEKG-DDKKQRKAVRFTRVQLLRPTENLVLG-HAYRLITSQEVMMKVLREKKSATKKHQ	115
at1g60010	ATTTTDDKSERKVVRFTRVKLLRPTEENLVLG-HAYRLITSQEVMMKVLRAKKYAKTKKHQ	113
at5g50090	TTALSSASSGHGGPLRLTRIKLLRPDTLVLG-HVYRLITKEVMKGLMAKKCSKLK--	104
at5g62900	SAVP-----HGGSLRVTRIKLLRPSDNLLG-HVYRLISSEEVMMKGIKAKKSGKMKKIH	100
at5g67620	SPTMK-----NEKGLPLKQLKLLRPDDTLIG-HVYRLVSFEEVLNEFATKKCVKLGKLL	102
at5g03890	THLLPDAKLLSGRLYYLLPTMTMKKKVNKKVT-FANPEVEGDERLLREEDSSESNSNID	105
at3G21680	-----EESKVVRKVVVTKKELRQILG-HKNGINSIQQLVHVLDKSGRNISMASY	95
at3G20340	-----DSKSSVPSHEIKIRLTKKQLHDLLS-KVN----VHDLTFQQQTFCPIILNNG	94
at4G21920	TSNVTSTSSSSSSERREIKIRITKKELEDLMRNIGLKSLTAEIILSKLIFEKGGDQIGFSA	108
G2	-----MKVKIVLTRHELDMLFLQMNRS-HDGNLMITKDVMMVELEKRIIRASSFSS	90

```

at1g10530 IEKTTT-----AKKFS-DKKVPEK-----KQGKQFR---VIRNSTSL 148
at1g60010 SETSKE-----KKKPSSEKKIDEESDKNQNLETKDEKQRS---VLTNAS- 155
at5g50090 -ESKGS-----DDKLEMVKAINSTKLDNEDQLQMKKQEK-----ER 139
at5g62900 GEFSVA-----EEEINPLTLRSESASDKDTQRRRIHEKQRG---MMNTGGA 142
at5g67620 KEGGGLDLTKKKTKHRKKKLDQETGKVNPNSDPNPNQDGADNAVAGENGSGFMRSHGG 162
at5g03890 GDDTKN-----VTVVRMKIVVHKQELEKLLQGGSVHEMMYQTLKQLLLTSSDDD 155
at3G21680 EEDEKE----- 101
at3G20340 YEEANQ----- 100
at4G21920 VDV TNH----- 114
G2 LSSSPS----- 96
.

```

III

```

at1g10530 LKQ-SKTWRPSLQSISEATS----- 167
at1g60010 -SR-SKTWRPSLQSISEATS----- 173
at5g50090 SRI-SRSWQPSLQSISEGGSS----- 159
at5g62900 TNK-VRAWQPSLQSISESTS----- 161
at5g67620 GRG-GGGWRPALHSIPEFGSS----- 182
at5g03890 DLECN SGWRPALDSIPESESLRRT-- 179
at3G21680 --EGDENWRPTLESIPESHY----- 119
at3G20340 ----QRLWRPVLQSIPEVN----- 115
at4G21920 ----HQPWKPVLSIPEMD----- 129
G2 ----SIAWEPALESILECPEVQEMDR 118
      * . * * . * * *

```

**Figure 3.21** ClustalW alignment of the deduced amino acid from the translation start sites of ORF among G2 and nine genes from *Arabidopsis*. “\*” indicates that the residues in that column are identical in all sequences in the alignment. “:” indicates that a conserved substitution has been observed. “.” Means that semi-conservative substitutions have been observed. I, III represent the two conserved motifs.

All the nine protein sequences are relatively short and have different expression profiles from the *Genevestigator\_V3* data. They were submitted to the online tool Myristoylator in ExPASy and the result showed that there were functionally unknown and involved in N-terminal protein myristoylation.

The protein sequences of the 9 potential homologues of G2 were also sent to TMHMM server 2.0 to predict potential transmembrane helices. Interestingly, same as G2, none of them contains any transmembrane helices.

Gene *At1g10530* is predicted to be expressed specifically in AZ, root tip and lateral root caps from Genevestigator\_V3 data, which suggests that it may play a role in cell separation. Gene *At1g10530* shares 73% genomic DNA sequence similarity with gene *At1g60010* and the latter is predicted to be expressed in all the tissues of *Arabidopsis*. Gene *At5g62900* is predicted to be expressed in all tissues, gene *At3g21680* is predicted to be expressed specifically in root tissues and gene *At2g20340* is predicted to be expressed specifically in chalazal seed coat.

### 3.4 Discussion

#### 3.4.1 Identification of *G2* as an abscission-related gene

Background research for this project identified 200 potential abscission-related genes with an abscission Affymetrix microarray data. Six genes of interest were identified for further study and the expression in AZ tissue was confirmed by RT-PCR analysis. In order to further investigate the spatial and temporal expression patterns of the six genes, the promoters were fused to the reporter GUS and GFP genes. GUS accumulation was identified at the base of sepals, petals and anther filaments at the stage when natural shedding took place. This project has focused on the characterization of one of the six genes which is *At1g64405* (*G2*).

Expression analysis of *G2* was carried out in *G2:GUS* homozygous transgenic lines. A strong *G2:GUS* signal was detected at the base of petals, sepals and anther filaments and the GUS expression extended into non-abscission zone cells, which might be the reason that GUS products spread through the vascular tissue. GUS accumulation commenced from flower position 6 – 7, which is consistent with other abscission-related genes such as *POLYGALACTURONASE ABSCISSION ZONE A. THALIANA* (*PGAZAT*) (Gonzalez-Carranza *et al.*, 2007; Ogawa *et al.*, 2009). The expression appeared to gradually decrease as the siliques developed.



To confirm that the expression of *G2* was specifically associated with abscission, three abscission-related mutants *inflorescence deficient in abscission (ida)*, *35S:IDA*, and *blade on petiole 1/2 (bop1/bop2)* were introduced to cross with *G2:GUS*. The *ida* mutant is deficient in floral organ abscission throughout pod maturation and dehiscence (Butenko, 2003). The breakstrength results showed that *ida* initially shared a reduction in breakstrength profile compared to wild type and then increased dramatically (Butenko, 2003). Compared with the *G2:GUS* signal in wild type, the expression of *G2:GUS* showed a slight delay, indicating the expression of *G2* is coordinated with the change in timing of abscission. Overexpression of *IDA* induces ectopic abscission of floral organs and shedding at a significantly earlier stage (position 4) than in wild type (Stenvik, 2006). The *35S:IDA* plants developed an ectopic AZ with highly increased numbers of separating cells (Stenvik, 2006). The *G2:GUS* signal displayed an earlier expression from position 4 compared with wild type in which the signal appeared at position 7 – 8. Moreover, *G2:GUS* expression was much stronger and covered the extended AZ cells though out the development of siliques. The genes *BLADE ON POTIOLE 1 and 2 (BOP1/BOP2)* have been showed to be crucial for floral AZ formation of *Arabidopsis* (Ha *et al.*, 2007, McKim *et al.*, 2008). Plants lacking *BOP1/BOP2* had been suggested to fail to differentiate an abscission zone (Hepworth *et al.*, 2005). *G2:GUS* was crossed with the double Knockout mutant *bop1/bop2* to investigate the *G2* expression in the mutants without the differentiation of AZ. GUS accumulation could only

be detected at low levels at position 10. This indicates that AZ differentiation does partially take place in *bop1/bop2* plants.

The conclusion for this study is that the spatial and temporal expression of G2 is correlated with abscission.

### **3.4.2 The expression of G2 is correlated with the expression shows an inverse correlation with *IDA*.**

The results presented in this chapter demonstrate that the spatial and temporal expression of G2 is correlated with the timing of abscission where in wild type this expression is observed at the floral stage immediately prior to organ shedding and this is delayed in *ida* and *bop1/bop2* plants whilst enhanced in *35S:IDA* plants. The expression detected in *bop1/bop2* suggests that some differentiation of the floral abscission zone takes place. Interestingly, G2 expression is also associated with lateral root emergence, which suggests that it could have a role in cell separation or protection against pathogens. The discovery that it is also up-regulated by wounding supports the latter role.

*IDA* has been reported to play an important role in lateral root development and is expressed in cortex and epidermal cells overlying lateral root primordia (Butenko *et al.*, 2010). *IDA* was also shown to be up-regulated by IAA. Both of these features are shared with G2 therefore

*IDA* and *G2* have a similar expression pattern expect that *G2* is wound-induced.

During the *G2:GUS* analysis, expression of *GUS* was observed to be associated with wounding of the flowers pedicels. Mutant analysis revealed that the wounding-induced expression was changed in an *ida* and *35S:IDA* background compared with wild type. In the *ida* background, the *G2:GUS* expression was up-regulated and more diffuse whereas in *35S:IDA* background, the *GUS* signal was no longer detectable.

*G2* reporter expression was also investigated in 7 day old root tissue. It was found that *G2:GUS* showed an expression in the cortical cells of adjacent to emerging lateral roots. In the absence of *IDA*, the *GUS* signal was more intense compared to wild type and extended from lateral root emergence sites to cover the whole root except the root tips. In the *35S:IDA* plants, *G2:GUS* expression was absent apart from weak expression at the root tips. The wounding-induced expression observation indicates that there is a negative correlation between *G2* and *IDA*. *G2* and *IDA* expression were then analysed *in silico* using the NASC array (<http://nasc.nottingham.ac.uk>) to gain information for the expression correlation between *G2* and *IDA* from microarray data. Microarray analysis provides an additional evidence of a negative correlation between *IDA* and *G2* expression.

Interestingly, in a *35S:IDA* background, *G2:GUS* signal was detected to be enhanced in AZ and root tips where cell separation takes place, whereas the wound-induced expression was decreased. This suggests that *G2* may play two distinct roles in cell separation and the protection against pathogens. *IDA* is clearly necessary for abscission to take place and overexpression of the protein leads to ectopic cell separation in AZ. *G2*, through its negative feedback role, could perhaps define the site of *IDA* expression. Further discussion of this suggestion will take place in the following chapters.

### **3.4.3 Transcription analysis of *G2* in *Arabidopsis* and sequence analysis of *G2* with putative orthologues in other species**

*G2* has an unknown function. Transcriptomic analysis showed that *G2* was highly expressed in AZ in the flowering stage, which has been confirmed by the expression analysis by fusing *G2* promoter with reporter genes *GUS* and *GFP*. Interestingly, Genevestigator\_V3 data showed that *G2* was relatively highly expressed in stamen, suggesting that *G2* may also play an important role in pollen development, which may be one of the reasons that down-regulating of *G2* leads to pollen grains that are partially undeveloped (see Chapter 4).

*G2* is a unique gene in *Arabidopsis thaliana*. Further TBLASTX results revealed four putative orthologues from four different plant species from

*Brassicaceae* family: *Arabidopsis lyrata*, *Brassica*, *Raphanus raphanistrum*, and *Raphanus sativus*. Alignment analysis of protein sequences by using ClustalW showed that the five deduced proteins including G2 are highly conserved in terms of amino acids homology.

Nineteen proteins from different plant species were identified by TBLASTX that share four conserved motifs in terms of amino acids similarity. The nineteen proteins were of similar size and relatively small. All of the proteins have a “MGNC” motif starts at the N’ terminus, following by 40 – 60 random amino acids, a conserved motif II (XKVKIVLXRXL), and ended with conserved motif III (WXPXLESIXE) in the C’ terminus. The results from ProtScale tool of ExPASy showed that all the twenty proteins have similar hydrophobicity scale. The results from TMHMM 2.0 server showed that none of them contained a transmembrane helix.

Although the major part of the protein sequences of the twenty proteins are unconserved, they show similar secondary structures in accordance to the results of PHYRE server. All of them contain an alpha helix motif near the N’ terminus, following a beta strand in motif II, and two motifs of alpha helixes in motif II and IV respectively. Amino acids in motif II are relatively conserved among the twenty proteins but in motif IV they are significantly varied. In a protein family, the core residues are often conserved and the loops are less conserved unless they play an important role in protein function (Levitt and Chothia, 1976), therefore the four motifs may serve as the functional domains in the twenty proteins.

The above results suggest that firstly, the twenty proteins including G2 may serve similar functions; secondly, the four motifs may play an important role in protein function.

The prediction of protein 3D structure showed that the deduced proteins in *Zea mays* and *Sorghum bicolor* contain spectrin repeat-like domains. In early studies, spectrin repeats have been shown to be involved in building long, extended molecules (Winder *et al.*, 1997). Recent studies support the hypothesis that spectrin repeats serve as a docking surface for cytoskeletal and signal transduction proteins (Djinovic-Carugo *et al.*, 2002). Homology analysis showed that G2 and the two deduced protein were potential homologues, therefore it is possible that G2 also contains a spectrin repeats domain. Spectrin repeats are often located in tissues that exposed to great mechanical stress such as the cell cortex (Lenne *et al.*, 2000). Expression analysis has shown that G2 is expressed in the cortical cells overlaying lateral root primordial and AZ cells, which are normally exposed under mechanical stress such as cell separation in lateral root emergence and organ shedding. Spectrin repeats have also been shown to have the ability to interact with many other proteins such as F-actin (Pascual *et al.*, 1996), which forms microfilaments, one of the three major components of cytoskeleton. In the actin binding process, spectrin repeats serve as a link between cytoskeleton and the plasma membrane (Djinovic-Carugo *et al.*, 2002). Ectopic expression of G2 leads to swollen root hairs in *Arabidopsis* (see Chapter 4), and the swollen root hairs can be one of

the effects of a disrupted cytoskeleton. If G2 is a spectrin repeat-like protein, it is possible that overexpression of G2 disrupts the F-actins. The binding list of the proteins that spectrin repeats can interact with is incomplete (Djinovic-Carugo *et al.*, 2002), therefore there is possibility that G2 could bind to IDA and IDLs, which would explain the phenotype in 35S:G2 and the cross homozygous of 35S:G2 x 35S:IDA (see Chapter 4). In future studies, Yeast two hybrid technologies might be used to test these interactions.

#### **3.4.4 Identification of 9 potential orthologues of G2 from *Arabidopsis thaliana***

The three identified motifs were then sent as probes to a online tool PetMatch in TAIR and the results revealed 9 genes in *Arabidopsis thaliana* that share motif I and III with G2. All of the 9 genes share the same N' terminus with four conserved amino acids "MGNC" (Motif I) and similar C' terminus (Motif III).

Interestingly, the 9 proteins share four similar features with G2. (1) The 10 proteins including G2 are in the similar size with the smallest one 115 amino acids and biggest one 182 amino acids. (2) Excluding G2 the rest of the 10 proteins are putatively involved in N-terminal protein myristoylation according to the information from TAIR. G2 was also predicted to be myristoylated by online tool Myristoylator in ExPASy. Myristoylation plays a vital role in membrane targeting and signal transduction in plant responses to environmental stress, which suggests

that G2 and the other 9 proteins may involved in stress response processes. (3) The 9 proteins sequences were sent to PHYRE online data base in order to predict protein secondary structures. Similar to G2, they all showed high content of helices. (4) The 9 proteins sequences were then sent to TMHMM Server 2.0 and the result showed that same as G2, none of them have any putative transmembrane helices.

The above evidence suggests that the identified 9 genes might have similar functions to G2. Together with G2 they may form a novel family of genes in which the two conserved motifs play an important role in protein function. To test this hypothesis, future work will be involved in the investigation of the function of the two motifs. For example, the cDNA of G2 without motif I or III in deduced protein sequence could be fused with G2 promoter, and then introduced into G2 null lines (T-DNA), in order to investigate whether absence of the two motifs can rescue the phenotype of *g2*. Alternatively, G2 protein without motif I or III could be fused with 35SCaMV promoter to investigate if G2 protein without these two motifs will bring about the swollen root hairs, which is described in Chapter 4 and is the consequence of ectopically expression of G2.